HHS Public Access

Author manuscript

Nat Hum Behav. Author manuscript; available in PMC 2017 October 24.

Published in final edited form as:

Nat Hum Behav. 2017 ; 1: . doi:10.1038/s41562-017-0069.

Evidence for a Large-Scale Brain System Supporting Allostasis and Interoception in Humans

Ian R. Kleckner[1,*], **Jiahe Zhang**[1], **Alexandra Touroutoglou**[2,3,4], **Lorena Chanes**[1,3,4], **Chenjie Xia**[3,5], **W. Kyle Simmons**[6,7], **Karen S. Quigley**[8,1], **Bradford C. Dickerson**[3,5,‡], and **Lisa Feldman Barrett**[1,3,4,*,‡]

[1]Department of Psychology, Northeastern University, Boston, MA

[2]Department of Neurology, Massachusetts General Hospital and Harvard Medical School

[3]Athinoula A. Martinos Center for Biomedical Imaging

[4]Psychiatric Neuroimaging Division, Department of Psychiatry, Massachusetts General Hospital and Harvard Medical School, Charlestown, MA

[5]Frontotemporal Disorders Unit, Department of Neurology, Massachusetts General Hospital and Harvard Medical School, Charlestown, MA

[6]Laureate Institute for Brain Research, Tulsa, OK

[7]School of Community Medicine, The University of Tulsa, Tulsa, OK

[8]Edith Nourse Rogers Memorial VA Hospital, Bedford, MA

Abstract

Large-scale intrinsic brain systems have been identified for exteroceptive senses (e.g., sight, hearing, touch). We introduce an analogous system for representing sensations from within the body, called interoception, and demonstrate its relation to regulating peripheral systems in the body, called allostasis. Employing the recently introduced Embodied Predictive Interoception Coding (EPIC) model, we used tract-tracing studies of macaque monkeys, followed by two intrinsic functional magnetic resonance imaging samples (N = 280 and N = 270) to evaluate the existence of an intrinsic allostatic/interoceptive system in the human brain. Another sample (N = 41) allowed us to evaluate the convergent validity of the hypothesized allostatic/interoceptive system by showing that individuals with stronger connectivity between system hubs performed better on an implicit index of interoceptive ability related to autonomic fluctuations. Implications include insights for the brain's functional architecture, dissolving the artificial boundary between mind and body, and unifying mental and physical illness.

[*]Corresponding authors: ian_kleckner@urmc.rochester.edu, l.barrett@neu.edu.
[‡]Shared senior authorship

Author contributions: The study was designed by all the authors, analyzed by all the authors, and the manuscript was written by I.R.K. and L.F.B with comments and edits from other authors.

Competing interests: The authors declare no competing interests.

The brain contains intrinsic systems for processing exteroceptive sensory inputs from the world, such as vision, audition, and proprioception/touch (e.g., [1]). Accumulating evidence indicates that these systems work via the principles of predictive coding (e.g., [2–7]), where sensations are anticipated and then corrected by sensory inputs from the world. The brain, as a generative system, models the world by *predicting*, rather than reacting to, sensory inputs. Predictions guide action and perception by continually constructing possible representations of the immediate future based on their prior probabilities relative to the present context[8,9]. We and others have recently begun studying the hypothesis that ascending sensory inputs from the organs and systems within the body's *internal milieu* are similarly anticipated and represented (i.e., autonomic visceral and vascular function, neuroendocrine fluctuations, and neuroimmune function)[10–16]. These sensations are referred to as *interoception*[17–19]. Engineering studies of neural design[20], along with physiological evidence[21], indicate that the brain continually anticipates the body's energy needs in an efficient manner and prepares to meet those needs before they arise (e.g., movements to cool the body's temperature before it gets too hot). This process is called *allostasis*[20–22]. Allostasis is not a condition or state of the body – it is the process by which the brain efficiently maintains energy regulation in the body. Allostasis is defined in terms of prediction, and recent theories propose that the prediction of interoceptive signals is necessary for successful allostasis (e.g., [10,15,23–25]). Thus, in addition to the ascending pathways and brain regions important for interoception (e.g., [17,18,26,27]), recent theoretical discussions (e.g., [11]) have proposed the existence of a distributed intrinsic allostatic/interoceptive system in the brain (analogous to the exteroceptive systems). A full investigation of the predictive nature of an allostatic/interoceptive brain system requires multiple studies under various conditions. Here, we identify the anatomical and functional substrates for a unified allostatic/interoceptive system in the human brain and reporting an association between connectivity within this system and individual differences in interoceptive-related behavior during allostatically relevant events.

In this paper, we first review tract-tracing studies of non-human animals that provide the anatomical substrate for our hypothesis that the brain contains a unified, intrinsic system for allostasis and interoception. Next, we present evidence of this hypothesized system in humans using functional connectivity analyses on three samples of task-independent (i.e., "resting state") functional magnetic resonance imaging (fMRI) data (also called "intrinsic" connectivity). We then present brain-behavior evidence to validate the hypothesized allostatic/interoceptive system by using an implicit measure of interoception during an allostatically challenging task. Finally, we summarize empirical evidence to show that this allostatic/interoceptive system is a *domain-general* system that supports a wide range of psychological functions including interoception, emotion, memory, reward, cognitive control, etc.[28,29]. That is, whatever else this system might be doing – remembering, directing attention, etc., – it is also predictively regulating the body's physiological systems in the service of allostasis to achieve those functions[23].

Our work synthesizes anatomical and functional brain studies that together evidence a single brain system – comprised of the salience and default mode networks – that supports not just allostasis but a wide range of psychological functions (emotion, pain, memory, decision-making, etc.) that can all be explained by their reliance on allostasis. To our knowledge, this evidence and our simple yet powerful explanation has not been presented despite the fact

that many functional imaging studies show that the salience and default mode networks support a wide range of psychological functions (i.e., they are domain general; e.g., [30]; for review, see [28,29]). Our paper provides the groundwork for a theoretical and empirical framework for making sense of these findings in an anatomically principled way. Our key hypotheses and results are summarized in Table 1.

Anatomical evidence supporting the proposed allostatic/interoceptive system

Over three decades of tract-tracing studies of the macaque monkey brain clearly demonstrate an anatomical substrate for the proposed flow of the brain's prediction and prediction error signals. Specifically, anatomical studies indicate a flow of information within the laminar gradients of these cortical regions according to the structural model of corticocortical connections developed by Barbas colleagues ([31]; for a review, see [32]). In addition, the structural model of corticocortical connections has been seamlessly integrated with a predictive coding framework[11,12]. Unlike other models of information flow that work in specific regions of cortex, the structural model successfully predicts information flow in frontal, temporal, parietal, and occipital cortices[33–37]. Accordingly, prediction signals flow from regions with less laminar development (e.g., agranular regions) to regions with greater laminar development (e.g., granular regions), whereas prediction error signals flow in the other direction. In our recently developed theory of interoception, called the Embodied Predictive Interoception Coding (EPIC) model[11], we integrated Friston's active inference approach to predictive coding[38–40] with Barbas's structural model to hypothesize that less-differentiated agranular and dysgranular visceromotor cortices in the cingulate cortex and anterior insula initiate visceromotor predictions through their cascading connections to the hypothalamus, the periaqueductal gray (PAG), and other brainstem nuclei known to control the body's internal milieu[41–44] (also see [32]; red pathways in Fig 1); simultaneously, the cingulate cortex and anterior insula send the anticipated sensory consequences of those visceromotor actions (i.e., interoceptive predictions) to the more granular primary interoceptive cortex in the dorsal mid to posterior insula (dmIns/dpIns[18,45,46] ; blue solid pathways; Fig 1). Using this logic, we identified a key set of cortical regions with visceromotor connections that should form the basis of our unified system for interoception and allostasis (we also included one subcortical region, the dorsal amygdala (dAmy), in this analysis due to the role of the central nucleus in visceromotor regulation; for details, see endnote 1). This evidence is summarized in Table 2. As predicted by our EPIC model, most of the key visceromotor regions in the proposed interoceptive system do, in fact, have monosynaptic, bidirectional connections to primary interoceptive cortex, reinforcing the hypothesis that they directly exchange interoceptive prediction and prediction error signals.

[1]We included the dAmy in our system because its central nucleus is known to have key visceromotor functions (for a review, see [153]); the dAmy, being a subcortical region, does not have a laminar structure, but there are connections between the amygdala and primary interoceptive cortex (dmIns/dpIns; e.g., [60,154,155]) that are predicted by the EPIC model (using Barbas's structural model of information flow within the cortex). Similarly, the anterior cingulate cortex (ACC), a key limbic visceromotor region, is connected with the amygdala in a pattern consistent with the EPIC model hypothesis that the ACC sends visceromotor prediction signals to the central nucleus (the ACC primarily sends output from its deep layers and receives input from the amygdala in its upper layers[156]). Currently, there are insufficient data to test the EPIC model hypothesis that amygdala projections terminate in the upper layers of dmIns/dpIns and receives inputs from its deep layers, as these data are not available in prior tract-tracing studies involving the insula and amygdala (e.g., [60,154,155]).

We also confirmed that these visceromotor cortical regions indeed monosynaptically project to the subcortical and brainstem regions that control the internal milieu (i.e., the autonomic nervous system, immune system, and neuroendocrine system), such as the hypothalamus, PAG, parabrachial nucleus (PBN), ventral striatum, and nucleus of the solitary tract (NTS) (Table 2, right column).

Next, we tested for evidence of these connections in functional data from human brains. Axonal connections between neurons, both direct (monosynaptic) and indirect (e.g., disynaptic) connections, are closely reflected in intrinsic brain systems (for a review, see [47,48]). As such, we tested for evidence of these connections in functional connectivity analyses on two samples of low-frequency Blood Oxygenation Level Dependent (BOLD) signals during task-independent (i.e., "resting state") fMRI scans collected on human participants (discovery sample, $N = 280$, 174 female, mean age = 19.3 years, SD = 1.4 years; replication sample, $N = 270{,}142$ female, mean age = 22.3 years, SD = 2.1 years). We then examined the validity of these connections in a third independent sample of participants ($N = 41$, 19 female, mean age = 33.5 years, SD = 14.1 years), following which we situated these findings in the larger literature on network function.

Results

Cortical and amygdalar intrinsic connectivity supporting a unified allostatic/interoceptive system in humans

Our seed-based approach estimated the functional connectivity between a set of voxels of interest (i.e., the seed) and the voxels in the rest of the brain as the correlation between the low-frequency portion of their BOLD signals over time, producing a discovery map for each seed region. Starting with the anatomical regions of interest specified by the EPIC model, and verified in the anatomical literature, we selected seed regions guided by previously published functional studies. We selected two groupings of voxels in primary interoceptive cortex (dpIns and dmIns) that consistently showed increased activity during task-dependent fMRI studies of interoception (Table 3, first and second rows). We selected seed regions for cortical visceromotor regions and the dAmy using related studies (Table 3, remaining rows). As predicted, the voxels in primary interoceptive cortex and visceromotor cortices showed statistically significant intrinsic connectivity (Fig. 2; replication sample Supplementary Figure 1). The dpIns was intrinsically connected to all visceromotor areas of interest (seven two-tailed, one-sample t-tests were each significant at $p < 10^{-7}$; Supplementary Table 1), and dmIns was intrinsically connected to most of them (Supplementary Table 1). The discovery and replication samples demonstrated high reliability for connectivity profiles of all seeds (η^2 mean = 0.99, SD = 0.004).

Next, we computed η^2 for all pairs of maps to determine their spatial similarity[49] (mean = 0.56, SD = 0.17), and then performed K-means clustering of the η^2 similarity matrix to determine the configuration of the system. Results indicated that the allostatic/interoceptive system is composed of two intrinsic networks connected in a set of overlapping regions (Fig. 3; replication sample, Supplementary Figure 2). The spatial topography of one network resembled an intrinsic network commonly known as the *default mode network* (Supplementary Figure 3 and Supplementary Figure 4; for a review, see [50]). The second

network resembled an intrinsic network commonly known as the *salience network* (Supplementary Figure 3 and Supplementary Figure 4; e.g., [51,52]), the cingulo-opercular network[53], or the ventral attention network[54]. Resemblance was confirmed quantitatively by comparing the percent overlap in our observed networks to reconstructions of the default mode and salience networks reported in Yeo, et al.[55] (Supplementary Table 2). Other cortical regions within the interoceptive system shown in Fig. 3 (e.g., dorsomedial prefrontal cortex, middle frontal gyrus), not listed in Table 2, support visceromotor control via direct anatomical projections to the hypothalamus and PAG (Supplementary Table 3), supporting our hypothesis that this system plays a fundamental role in visceromotor control and allostasis.

Subcortical, hippocampal, brainstem, and cerebellar connectivity supporting a unified allostatic/interoceptive system in humans

Using a similar analysis strategy, we assessed the intrinsic connectivity between the cortical and dorsal amygdalar seeds of interest and the thalamus, hypothalamus, cerebellum, the entire amygdala, hippocampus, ventral striatum, PAG, PBN, and NTS. The observed functional connections with these cortical and amygdalar seeds, which regulate energy balance, strongly suggest that the proposed allostatic/interoceptive system itself also regulates energy balance (see Supplementary Discussion for details). All results replicated in our independent sample ($N = 270$; Supplementary Figure 5, η^2 mean = 0.98, SD = 0.008). Fig. 4 illustrates the connectivity between default mode and salience networks and the non-cortical targets in the discovery sample. Supplementary Figure 6 shows connectivity between the individual cortical and amygdalar seed regions listed in Table 2. We also observed specificity in the proposed allostasis/interoception system: non-visceromotor brain regions that are unimportant to interoception and allostasis, such as the superior parietal lobule (Supplementary Figure 7), did not show functional connectivity to the subcortical regions of interest.

The cortical hubs of the allostatic/interoceptive system also overlapped in their connectivity to non-cortical regions involved in allostasis (purple in Fig. 4), including the dAmy, the hypothalamus, the PBN, and two thalamic nuclei – the VMpo and both the medial and lateral sectors of the mediodorsal nucleus (MD, which shares strong reciprocal connections with medial and orbital sectors of the frontal cortex, the lateral sector of the amygdala, and other parts of the basal forebrain; for a review, see [56]). Additionally, the connector hubs also shared projections in the cerebellum and hippocampus (see Fig. 4).

Taken together, our intrinsic connectivity analyses failed to confirm only five monosynaptic connections (8%) that were predicted from non-human tract-tracing studies: hypothalamus-dAmy, hypothalamus-dpIns, PAG-dAmy, PAG-medial ventral anterior insula (mvaIns), and NTS-subgenual anterior cingulate cortex (sgACC). This is approximately what we would expect by chance; however, there are several factors that might account for why these predicted connections did not materialize in our discovery and replication samples. First, all discrepancies involved the sgACC, PAG, or hypothalamus, whose BOLD data exhibit poor signal to noise ratio due to their small size and their proximity to white matter or pulsating ventricles and arteries[57]. Second, individual differences in anatomical structure can make

inter-subject alignment challenging, particularly in 3-T imaging of the brainstem where clear landmarks are not always available. Of the connections that did not replicate, one involved the anterior insula; there is some disagreement in the macaque anatomical literature as to the exact location of the anterior insula (e.g., [45,58–60]), which might help explain any lack of correspondence between intrinsic and tract-tracing findings that we observed.

Validating the functions of the allostatic/interoceptive system in humans

The allostatic/interoceptive system reported in Fig. 3 replicated in the validation sample (η^2 mean = 0.84, SD = 0.05 compared with discovery sample cortical maps; η^2 mean = 0.76, SD = 0.07 compared with discovery sample subcortical maps). These η^2 values are respectable and demonstrate adequate reliability of the system according to conventional psychometric theory, although the lower η^2 values are likely due to the smaller sample size which magnifies the effects of poor signal-to-noise ratio in subcortical regions. Convergent validity for the proposed allostatic/interoceptive system was demonstrated in that individuals with stronger functional connectivity within the system also reported greater arousal while viewing images that evoked greater sympathetic nervous system activity. Participants viewed ninety evocative photos known to induce a range of autonomic nervous system changes and corresponding feelings of arousal[61], as well as changes in BOLD activity within these regions[62,63]. We predicted, and found, that individuals showing stronger intrinsic connectivity within the allostatic/interoceptive system (specifically, connectivity between dpIns and anterior midcingulate cortex (aMCC)) also demonstrated a stronger concordance between objective and subjective measures of bodily arousal while viewing allostatically relevant images ($p = 0.003$; see Supplementary Figure 8; see Supplementary Discussion for details).

There were three reasons for demonstrating the convergent validity of the proposed allostatic/interoceptive system using this task. First, there is a decades-old body of research indicating that interoception enables the subjective experience of arousal ([64]; e.g., [65,66]). Thus, the amount of joint information shared by an objective, psychophysiological measure of visceromotor change (skin conductance) and the subjective experience of arousal (self-report ratings) is an implicit, behavioral measure of interoceptive ability. Indeed, individuals with more accurate interoceptive ability exhibit a stronger correspondence between subjective arousal and physiological arousal in response to similar evocative photos[67]. Second, explicit reports of interoceptive performance on heartbeat detection tasks (e.g., [68–70]) are complex to interpret neutrally because they require synthesizing and comparing information from other systems (somatosensory system[71], frontoparietal control systems, and, for heartbeat detection, the auditory system); in addition, these tasks are sometimes too hard (yielding floor effects) or have questionable validity[70].

At this juncture, it is tempting to ask if the unified allostatic/interoceptive system is specific to allostasis and interoception. From our perspective, this is the wrong question to be asking. The last two decades of neuroscience research have brought us to the brink of a paradigm shift in understanding the workings of the brain, setting the stage to revolutionize brain: mind mapping. Neuroscience research is increasingly acknowledging that brain networks have a one (network) to many (function) mappings[28–30,72–74]. Our findings contribute to this

discussion: a brain system that is fundamental to allostasis and interoception is not unique to those functions, but instead is also important for a wide range of psychological phenomena that span cognitive, emotional, and perceptual domains (Fig. 5.). This finding is not a failure of reverse inference. It suggests a functional feature of how the brain works.

Discussion

The integrated allostatic/interoceptive brain system is a complex cortical and subcortical system consisting of connected intrinsic networks. Our work demonstrates a single brain system that supports not just allostasis but also a wide range of psychological phenomena (emotions, memory, decision-making, pain) that can all be explained by their reliance on allostasis. Other studies have already shown that regions controlling physiology are also regions that control emotion. In fact, this was Papez's original logic for assuming that the "limbic system" was functionally for emotion. This paper goes beyond this observation. Regions controlling and mapping of inner body physiology lie in networks that also social affiliation, pain, judgments, empathy, reward, addiction, memory, stress, craving, decision making, etc. (Fig. 5). More and more, functional imaging studies are finding that the salience and default mode networks are domain-general (e.g., [30]; for review, see [28,29]). Our paper provides the groundwork for a theoretical and empirical framework for making sense of these findings in an anatomically principled way.

Our investigation was strengthened by our theoretical framework (the EPIC model[11]), the converging evidence from structural studies of the brain (i.e., tract-tracing studies in monkeys plus the well-validated structural model of information flow), our use of multiple methods (intrinsic connectivity in humans, as well as brain-behavior relationships), and our ability to replicate the system in three separate samples totaling over 600 human participants. Our results are consistent with prior anatomical and functional studies that have investigated portions of this system at cortical and subcortical levels (e.g., [17,18,26,27,75–78]), including evidence that limbic cortical regions control the brainstem circuitry involved with allostatic functions such as cardiovascular control, respiratory control, and thermoregulatory control[79], as well as prior investigations that focused on the intrinsic connectivity of individual regions such as the insula (e.g., [80]), the cingulate cortex (e.g., [81]), the amygdala (e.g., [82]), and the ventromedial prefrontal cortex (e.g., [83]); importantly, our results go beyond these prior studies in several ways. First, we observed an often-overlooked finding when interpreting the functional significance of certain brain regions: the dorsomedial prefrontal cortex, the ventrolateral prefrontal cortex, the hippocampus, and several other regions have both a structural and functional pattern of connectivity that indicates their role in visceromotor control. A second often-overlooked finding is that relatively weaker connectivity patterns (e.g., between the visceromotor sgACC and primary interoceptive cortex) are reliable, and future studies may find that they are of functional significance. Third, we demonstrated behavioral relevance of connectivity within this network, something that prior studies of large-scale autonomic control networks have yet to test (e.g., [75–77]). Taken together, our results strongly support the EPIC model's hypothesis that visceromotor control and interoceptive inputs are integrated within one unified system[11], as opposed to the traditional view that the cerebral cortical regions sending visceromotor signals and those that

receive interoceptive signals are organized as two segregated systems, similar to the corticospinal skeletomotor efferent system and the primary somatosensory afferent system.

Perhaps most importantly, the allostatic/interoceptive system has been shown to play a role in a wide range of psychological phenomena, suggesting that allostasis and interoception are fundamental features of the nervous system. Anatomical, physiological, and signal processing evidence suggests that a brain did not evolve for rationality, happiness, or accurate perception; rather, all brains accomplish the same core task[20]: to efficiently ensure resources for physiological systems within an animal's body (i.e., its internal milieu) so that an animal can grow, survive, thrive, and reproduce. That is, the brain evolved to regulate *allostasis*[21]. All psychological functions performed in the service of growing, surviving, thriving, and reproducing (such as remembering, emoting, paying attention, deciding, etc.) require the efficient regulation of metabolic and other biological resources.

Our findings add an important dimension to the existing observations that the default mode and salience networks serve as a high-capacity backbone for integrating information across the entire brain[84]. Diffusion tensor imaging studies indicate, for example, that these two networks contain the highest proportion of hubs belonging to the brain's "rich club," defined as the most densely interconnected regions in the cortex[73,85] (several of which are connector hubs within the allostatic/interoceptive system; see Fig. 3, Supplementary Table 4). All other sensory and motor networks communicate with the default mode and salience networks, and potentially with one another, through these hubs[1,85]. The agranular hubs within the two networks, which are also visceromotor control regions, are the most powerful predictors in the brain[11,32]. Indeed, hub regions in these networks display a pattern of connectivity that positions them to easily send prediction signals to every other sensory system in the brain[12,32].

The fact that default mode and salience networks are concurrently regulating and representing the internal milieu, while they are routinely engaged during a wide range of tasks spanning cognitive, perceptual, and emotion domains, all of which involve value-based decision-making and action[86] (e.g., [87–90; 30;] for a review, see [88]), suggest a provocative hypothesis for future research: whatever other psychological functions the default mode and salience networks are performing during any given brain state, they are simultaneously maintaining or attempting to restore allostasis and are integrating sensory representations of the internal milieu with the rest of the brain. Therefore, our results, when situated in the published literature, suggest that the default mode and salience networks create a highly connected functional ensemble for integrating information across the brain, with interoceptive and allostatic information at its core, even though it may not be apparent much of the time.

When understood in this framework, our current findings do more than just pile on more functions to the ever-growing list attributed to the default mode and salience networks (which currently spans cognition, attention, emotion, perception, stress, and action; see [28,30]). Our results offer an anatomically plausible computational hypothesis for a set of brain networks that have long been observed but whose functions have not been fully understood. The observation that allostasis (regulating the internal milieu) and interoception

(representing the internal milieu) are at the anatomical and functional core of the nervous system[18,20] further offer a generative avenue for further behavioral hypotheses. For example, it has recently been observed that many of the visceromotor regions within the unified allostatic/interoceptive system contribute to the ability of S*uperAgers* to perform memory and executive function tasks like young[91].

Furthermore, our findings also help to shed light on two psychological concepts that are constantly confused in the psychological and neuroscience literatures: affect and emotion. If, whatever else your brain is doing—thinking, feeling, perceiving, moving—it is also regulating your autonomic nervous system, your immune system, and your endocrine system, then it is also continually representing the interoceptive consequences of those physical changes. Interoceptive sensations are usually experienced as lower-dimensional feelings of affect[92,93]. As such, the properties of affect—valence and arousal[94,95]—can be thought of as basic features of consciousness[96–102] that, importantly, are not unique to instances of emotion.

Perhaps the most valuable aspect of our findings is their value for moving beyond traditional domain-specific or "modular" views of brain structure/function relationships[103], which assume a significant degree of specificity in the functions of various brain systems. A growing body of evidence requires that these traditional modular views be abandoned[28,104,105] in favor of models that acknowledge that neural populations are domain-general or multi-use. The idea of domain-generality even applies to primary sensory networks, as evidenced by the fact that multisensory processing occurs in brain regions that are traditionally considered unimodal (e.g., auditory cortex responding to visual stimulation[106,107]). The absence of specificity in brain structure/function relationships is not a measurement error or some biological dysfunction, but rather it is a useful feature that reflects core principles of biological degeneracy that are also evident in the genome, the immune system, and every other biological system shaped by natural selection[108].

No study is without limitations. First, there are potential issues identifying homologous regions between monkey and human brains[47]; nonetheless, we still found evidence for the majority of the monosynaptic connections predicted by the EPIC model. Second, we used an indirect measure of brain connectivity in humans (functional connectivity analyses of low-frequency BOLD data acquired at rest) that reflects both direct and indirect connections and can, in principle, inflate the extent of an intrinsic network[47]. Moreover, low frequency BOLD correlations may reflect vascular rather than neural effects in brain[109]. Nonetheless, our results exhibit specificity: the integrated allostatic/interoceptive system conforms to well-established salience and default mode networks and is remarkably consistent with both cortical and subcortical connections repeatedly observed in tract-tracing studies of non-human animals. Third, although our fMRI procedures were not optimized to identify subcortical and brainstem structures and study their connectivity (e.g., [57,75,76,110]), we nonetheless observed 92% of the predicted connectivity results. Finally, many studies find that activity in the default mode and salience networks have an inverse or negative relationship (sometimes referred to as "anti-correlated"), meaning that as one network increases its neural activity relative to baseline, the other decreases. Such findings and interpretations have recently been challenged on both statistical and theoretical grounds

(e.g., [111]; see Supplementary Discussion). In fact, when global signal is not removed in pre-processing, the two networks can show a pattern of positive connectivity (e.g., [112]). Fourth, our demonstration of a brain/behavior relationship (using the evocative pictures) was merely a preliminary evaluation of how individual differences in the function of this system are related to individual differences in behavior. Additionally, our use of electrodermal activity as a measure of sympathetic nervous system activity is arguably too specific because different components of the sympathetic nervous system react differently[113], and peripheral sensations associated with changes in electrodermal activity might not be processed by the interoceptive brain circuitry that we are studying here, thus complicating the interpretation of our results. However, we did not intend to assess any particular path carrying information about electrodermal activity specifically, and we believe that – despite their limitations – our results are still useful and hypothesis-generating. Future work will be needed to understand this and other brain/behavior relationships involving this system more thoroughly.

This work one in a series of future studies to precisely test the EPIC model, including its predictive coding features (not just the anatomical and functional correlates as shown here). Future research must focus on the ongoing dynamics by which the default mode and salience networks support allostasis and interoception, including the predictions they issue to other sensory and motor systems. It is possible, for example, that both networks use past experience in a generative way to issue prediction signals, but that the default mode network generates an internal model of the world via multisensory predictions (consistent with [114–116]), whereas the salience network issues predictions, as precision signals, to tune this model with prediction error (consistent with the salience network's role in attention regulation and executive control; e.g., [51,117,118]). Unexpected sensory inputs that are anticipated to have allostatic implications (i.e., likely to impact survival, offering reward or threat) will be encoded as "signal" and learned to better support allostasis in the future, with all other prediction error is treated as "noise" and safely ignored ([119]; for discussion, see [120]). These and other hypotheses regarding the flow of predictions and prediction errors in the brain (e.g., incorporating the cerebellum, ventral striatum, and thalamus[24] can be tested using new methods such laminar MRI scanning at high (7 T) magnetic field strengths (e.g., [121]).

Future research that provides a more mechanistic understanding of how the default mode and salience networks support interoception and allostasis will also reveal insights into the mind-body connections at the root of mental and physical illness and their comorbidities. For example, in illness, the neural representations of the world that underlie action and experience may be directed more by predicted allostatic relevance of information than by the need for accuracy and completeness in representing the environment. Indeed, atrophy or dysfunction within parts of the interoceptive system are considered common neurobiological substrates for mental and physical illness[122–124], including depression[125], anxiety[126], addiction[127], chronic pain[128], obesity[129], and chronic stress[130,131]. By contrast, increased cortical thickness in MCC is linked to the preserved memory of S*uperAgers* relative to their more typically performing elderly peers[132,133], suggesting a potential mechanism for how exercise (via the sustained visceromotor regulation it requires) benefits cognitive function in aging[134] and why certain activities, such as mindfulness or contemplative practice, can be beneficial (e.g., [135,136]). Ultimately, a better understanding of how the mind is linked to the

physical state of the body through allostasis and interoception may help to resolve some of the most critical health problems of our time, such as the comorbidities among mental and physical disorders related to metabolic syndrome (e.g., depression and heart disease[137]), or how chronic stress speeds cancer progression[138], as well as offer key insights into how an opioid crisis[139] and recorded numbers of suicides[140] emerge.

Methods

Participants

Discovery and replication samples—We randomly selected 660 participants (365 female, 55%, 18–30 years) from 1,000 healthy participants described in Yeo, et al.[55,141]. The 1,000 participants were native English-speaking adults, 18–35 years, with normal or corrected-to-normal vision, and reported no history of neurological or psychiatric conditions. We removed 79 participants (11%) due to head motion and outlying voxel intensities; we removed 31 more participants (4.7%) due to lack of signal in superior and lateral parts of the brain (see Analysis section). Our final dataset of 550 participants was randomly divided into a discovery sample of N=280 (174 female, 62%, mean=19.3 years, SD=1.4 years) and a replication sample of N=270 (142 female, 53%, mean=22.3 years, SD=2.1 years).

We also randomly selected 150 participants (75 female, 50%, mean=22.5, SD=2.0 years) from the N=1,000 to generate maps of the established default mode and salience networks.

Validity sample—We selected all 66 young and middle aged participants (33 female, 18–60 years, mean=34.8 years, SD=13.8 years) from an existing dataset of 111 participants (56 female, 18–81 years, mean=46.6 years, SD=18.9 years) recruited from the Boston area during 2012–2014 for a study examining age-related changes in how affect supports memory[142]. Only 41 participants (14 female, 47%, 20–60 years, mean=33.8 years, SD=14.1 years) had both high-quality fMRI BOLD data and sufficient electrodermal activity changes according to previously established procedures (see Analysis section). Specifically, 12 participants exhibited excessive head motion and outlying voxel intensities, and 16 participants lacked electrodermal responses. Participants were right-handed, native English speakers and had normal or corrected-to-normal vision. None reported any history of neurologic or psychiatric condition, learning disability or serious head trauma. Participants did not smoke and did not ingest substances that interfere with autonomic responsiveness (e.g., beta-blockers, anti-cholinergic medications).

Sample size—No pre-specified effect size was known, so we used a large portion of a third-party dataset (N=660) and the maximum size of a second dataset collected in our lab with young and middle-aged adults (N=66).

Procedure

Discovery and replication samples—Participants provided written informed consent in accordance with the guidelines set by the institutional review boards of Harvard University or Partners Healthcare. Participants completed MRI structural and resting state

scans and other tasks unrelated to the current analysis. MRI data were acquired at Harvard and the Massachusetts General Hospital across a series of matched 3T Tim Trio scanners (Siemens, Erlangen, Germany) using a 12-channel phased-array head coil. Structural data included a high-resolution multiecho T1-weighted magnetization-prepared gradient-echo image (multiecho MP-RAGE). Parameters for the structural scan were as follows: repetition time (TR)=2,200 ms, inversion time (TI)=1,100 ms, echo time (TE)=1.54 ms for image 1 to 7.01 ms for image 4, flip angle (FA)=7°, 1.2×1.2×1.2-mm voxels, and field of view (FOV)=230 mm. The functional resting state scan lasted 6.2 min (124 time points). The echo planar imaging (EPI) parameters for functional connectivity analyses were as follows: TR=3,000 ms, TE=30 ms, FA=85°, 3×3×3-mm voxels, FOV=216 mm, and 47 axial slices collected with interleaved acquisition and no gap between slices.

Validity sample—Participants were consented in accordance with the institutional review board. Data were acquired on separate sessions across several days. The first session consisted of a 6-min seated baseline assessment of peripheral physiology, the EXAMINER cognitive battery[143], a second 6-min seated baseline, the evocative images task, and other tasks. Only the evocative images task is relevant for this study. Electrodes were placed on the chest, hands, and face to record electrocardiogram, electrodermal activity, and facial electromyography, respectively. A belt with a piezoelectric sensor was secured on the chest to record respiration. Only the electrodermal activity data are reported here. Electrodermal activity was recorded using disposable electrodermal electrodes (containing isotonic paste) affixed to the thenar and hypothenar eminences of the left hand. Data were collected using BioLab v3.0.13 (Mindware Technologies, Gahanna, OH, USA). Participants sat upright in a comfortable chair in a dimly lit room. Ninety full-color photos were selected from the International Affective Picture System (IAPS) and used to induce affective experiences[61]. The pictures were selected based on normative ratings of pleasure/displeasure (valence) and arousal experienced when viewing them (i.e. unpleasant-high arousal, pleasant-high arousal, unpleasant-low arousal, pleasant-low arousal, neutral valence-low arousal; Supplementary Table 5). Participants viewed the photos sequentially on a 120×75 cm high-definition screen two meters away. Photos were grouped into three blocks of thirty each, with the order of the photos within each block fully randomized. For each trial, participants viewed an IAPS photo for six seconds, and then rated their experience for valence and arousal using the Self Assessment Manikin (SAM[144]). Only the arousal ratings are relevant to this report and they ranged from 1 (“Very calm”) to 5 (“Very activated”). A variable inter-trial interval of 10–15 seconds followed the rating prior to presentation of the next picture. Before beginning the task, participants were familiarized with the SAM rating procedure and practiced by rating five pictures. The photos and rating scales were administered via E-Prime (Psychology Software Tools, Pittsburgh, PA).

The second laboratory testing session involved MRI scanning, consisting of a structural scan, resting state scan, and other tasks unrelated to the present report (presented elsewhere[142]). MRI data were acquired using a 3T Tim Trio scanner (Siemens, Erlangen, Germany) using a 12-channel phased-array head coil. Structural data included a high-resolution T1-weighted MP-RAGE with TR=2,530 ms, TE=3.48 ms, FA=7°, and 1×1×1-mm isotropic voxels. The functional resting state scan lasted 6.40 min (76 time points). The EPI

parameters were as follows: TR=5,000 ms, TE=30 ms, FA=90°, 2×2×2-mm voxels, and 55 axial slices collected with interleaved acquisition and no gap between slices. Participants were instructed to keep their eyes open without fixating and remain as still as possible.

Analysis of task-independent ("resting state") fMRI data

Quality assessment—We applied established censoring protocols for head motion and outlying signal intensities using AFNI (https://afni.nimh.nih.gov/afni/) following Jo, et al. [145] and described in the following three steps: First, we disqualified an fMRI volume if AFNI's *enorm motion* derivative parameter (derived from *afni_proc.py*) was greater than 0.3 mm. Second, we disqualified an fMRI volume if the fraction of voxels with outlying signal intensity (AFNI's *3dToutcount* command) was greater than 0.05. Third, if a volume surpassed either criterion, we removed that volume, the prior volume, and the next two volumes. In a separate procedure, we disqualified discovery and replication participants who lost more than 10% of their 124 volumes due to either criterion (79 participants, 11%). Quality assessment for surface-based processing required removing 31 additional participants (4.7%) due to a lack of signal in the most superior and lateral parts of the brain, which would result in incomplete group connectivity maps; no participants were removed for this reason in the validity sample. In the validity sample, we removed participants who lost more than 40% of their 76 volumes, removing 12 participants (18%); we used a more lenient threshold due to the small sample size (N=66). The fraction of volumes censored per participant using the aforementioned approach by Jo, et al.[141] yielded nearly identical results to another established censoring approach described in Power, et al. [146] as implemented in AFNI's *afni_restproc.py* script.

Preprocessing—We applied standard Freesurfer preprocessing steps to both samples of resting state data (http://surfer.nmr.mgh.harvard.edu). These included removal of the first four volumes, motion correction, slice timing correction, resampling to the MNI152 cortical surface (left and right hemispheres) and MNI305 subcortical volume (2 mm isotropic voxels), spatial smoothing (6 mm FWHM, surface and volume separately) and temporal filtering (0.01 Hz high-pass filter and 0.08 Hz low-pass filter). We did not use global signal regression as to prevent spurious negative correlations ("anti-correlated networks"), which can interfere with interpreting the connectivity results[111].

Functional connectivity analysis—We estimated cortical connectivity using surface-based analyses, affording more sensitive and reliable discovery maps and reducing artifacts around sulcal and opercular borders by registering each participant's native space to MNI152 space via Freesurfer's reconstruction of each participant's cortical surfaces[147]. The surface-based intrinsic analyses also allowed us to incorporate the selected subcortical seed (dAmy), but did not allow us to analyze connectivity to subcortical structures more broadly. We first created a 4-mm radius sphere centered on the MNI coordinates identified in Table 3 and found the vertex on the MNI152 pial surface that is closest to the spherical seed. We then smoothed this single vertex by 4 mm on the surface and mapped the resulting cortical label to each individual subject's cortex. The individual cortical label was projected back into the subject's native volumetric space to calculate the averaged time series within the seed. For the subcortical seed (dAmy), we directly projected the spherical seed into each

subject's native volumetric space and extracted its time course. On the subject level, we ran a voxel-wise regression on left and right hemispheres of MNI152 and subcortical volume of MNI305 to compute the partial correlation coefficient and correlation effect size of the seed time series, taking into account several nuisance variables: cerebrospinal fluid signal, white matter signal, motion correction parameters, and a 5th order polynomial. On the group level, we concatenated the contrast effect size maps from all subjects and ran a general linear model analysis to test if the group mean differed from zero. This yielded final group maps that showed regions whose fluctuations significantly correlated with the seed's BOLD time series.

To estimate cortical-subcortical connectivity, we used a more liberal statistical threshold compared to the analyses of corticocortical connectivity. The smaller size of subcortical regions, as well as their anatomical placement, renders their signal noisier and less reliable[57], yielding relatively smaller estimates of intrinsic connectivity. Thus, guided by classical measurement theory[148], we relied on replication to determine which connectivity values were meaningful.

K-means cluster analysis of discovery maps—First, we computed the 8x8 η^2 similarity matrix for each pair of maps[49]. Based on visual inspection of the eight maps, we used K-means clustering with k=2 and k=3 using the *kmeans* function in MATLAB (Mathworks, Natick, MA). Our results confirmed that k=2 captured the default mode versus salience distinction across these maps, whereas k=3 further divided the 'salience cluster' into two sub-categories depending on whether or not somatosensory cortices are included. Because sub-categories within the salience network were not important to our study goals, we used the k=2 cluster solution.

Identification of the interoceptive system networks—We confirmed that Network 1 is the established default mode network (for a review, see [50]) and Network 2 is the established salience network[51,52]. The reference maps were constructed using coordinates obtained from Yeo, et al.[55] as follows. Using a random sample of N=150, we created a mask of the default mode network by conjoining functional connectivity maps from two hubs in the default mode network[55]: a 4-mm seed at the dorsomedial prefrontal cortex (MNI 0, 50, 24) and a 4-mm seed at the posterior cingulate cortex (MNI 0, −64, 40). We likewise created a mask of the salience network by conjoining functional connectivity maps from two bilateral hubs in the salience network (labeled as the ventral attention network in Yeo, et al.[55]): 4-mm seeds at the left and right supramarginal gyrus (MNI ±60, −30, 28) and 4-mm seeds at the left and right anterior insula (MNI ±40, 12, −4). We thresholded our maps to $p < 10^{-5}$ uncorrected (as in all our analyses) and we thresholded the default mode and salience networks to $z(r) > 0.05$ where z is the Fisher's r-to-z transformation. We then calculated the percent of each established network (default mode or salience) that covered each of our networks (Network 1 or 2), and the complementary measure: the percentage of each of our networks (Network 1 or 2) that covered each established network (default mode or salience). These calculations used only the right hemisphere.

Reliability analyses—We used η^2 as an index of reliability because it shows similarity between maps while discounting scaling and offset effects[49]. An η^2 value of 1 indicates

spatially identical maps, while an η^2 value of 0.5 indicates statistically independent maps. For each of our eight cortical and amygdalar seeds, we calculated η^2 between the discovery and replication samples using the effect size (gamma) maps generated by the group-level general linear model analysis. Then we calculated the mean and SD of the eight η^2 values across all seeds to index overall similarity between samples. This was done separately for the cortical and subcortical maps. We repeated the same procedure to compare the reliability between the discovery and validation samples.

Analysis of the evocative images task

We analyzed electrodermal activity data using Electrodermal Activity Analysis v3.0.21 (Mindware). For each 6-second trial when the photo was visible, we measured the number of event-related skin conductance responses (SCRs) according to best practices[149]. We considered an SCR to be event-related if both the response onset and peak occurred between 1 and 6 seconds after stimulus onset, with an amplitude ≥0.01 μS. It is commonly observed that a substantial proportion of healthy adults produce relatively few if any SCRs[150]. We disqualified 16 of our 66 participants (24%) because they generated event-related SCRs during fewer than 5% of the evocative photo trials. We analyzed our data using the number of SCRs (as opposed to the amplitude of the SCRs) per prior work from our group (e.g., [151]) and others (e.g., [152]).

Multilevel linear modeling to assess correspondence between objective physiological and subjective arousal during an allostatically relevant task—We used HLM v7.01 with robust parameter estimates (Scientific Software International; Skokie, IL). Level-1 of the model estimated the linear relationship (slope and intercept) between physiological arousal (number of event-related SCRs) and subjective arousal (1="Very calm" to 5="Very activated") in response to each of ninety photos. Thus, the model was adjusted for mean individual reactivity. Level-2 estimated the extent to which intrinsic connectivity between viscerosensory and visceromotor regions (e.g., dpIns-aMCC) moderated the relationship between objective and subjective arousal (i.e., moderated the slope of the Level 1 model). All variables were unstandardized. Level-1 variables were group-mean centered (for each participant) and Level-2 variables were grand-mean centered (across participants).

Data availability—The data that support the findings of this study are available from the corresponding author upon request.

Code availability—The code to analyze data are available from the corresponding author upon request.

Supplementary Material

Refer to Web version on PubMed Central for supplementary material.

Acknowledgments

The authors acknowledge Miguel Angel Garcia-Cabezas for comments and advice on neuroanatomy and Henry Evrard for helpful discussions on anatomical connectivity. This research was supported by funds from the National

Institutes on Aging (R01 AG030311) to L.F.B. and B.C.D., the US Army Research Institute for the Behavioral and Social Sciences Contracts (W5J9CQ-11-C-0046 and W5J9CQ-12-C-0049) to L.F.B., the National Institute of Mental Health Ruth L. Kirschstein National Research Service Award (F32MH096533) to I.R.K., the National Cancer Institute (UG1 CA189961 and R25 CA102618) to support I.R.K., the National Institutes of Mental Health (K01MH096175-01) and Oklahoma Tobacco Research Center grants to W.K.S, and the Fonds de recherche sante Quebec fellowship award to C.X. The views, opinions, and/or findings contained in this paper are those of the authors and shall not be construed as an official Department of the Army position, policy, or decision, unless so designated by other documents. The funders had no role in study design, data collection and analysis, decision to publish, or preparation of the manuscript

References and Notes

1. Sepulcre J, Sabuncu MR, Yeo TB, Liu H, Johnson KA. Stepwise connectivity of the modal cortex reveals the multimodal organization of the human brain. J Neurosci. 2012; 32:10649–10661. [PubMed: 22855814]
2. Rao RP, Ballard DH. Predictive coding in the visual cortex: A functional interpretation of some extra-classical receptive-field effects. Nat Neurosci. 1999; 2:79–87. [PubMed: 10195184]
3. Chennu S, et al. Expectation and attention in hierarchical auditory prediction. J Neurosci. 2013; 33:11194–11205. [PubMed: 23825422]
4. Shipp S. The importance of being agranular: A comparative account of visual and motor cortex. Philos Trans R Soc Lond B Biol Sci. 2005; 360:797–814. [PubMed: 15937013]
5. Zelano C, Mohanty A, Gottfried JA. Olfactory predictive codes and stimulus templates in piriform cortex. Neuron. 2011; 72:178–187. [PubMed: 21982378]
6. Kusumoto-Yoshida I, Liu H, Chen BT, Fontanini A, Bonci A. Central role for the insular cortex in mediating conditioned responses to anticipatory cues. Proc Natl Acad Sci U S A. 2015; 112:1190–1195. [PubMed: 25583486]
7. Adams RA, Shipp S, Friston KJ. Predictions not commands: Active inference in the motor system. Brain structure & function. 2013; 218:611–643. [PubMed: 23129312]
8. Clark A. Whatever next? Predictive brains, situated agents, and the future of cognitive science. Behav Brain Sci. 2013; 36:181–204. [PubMed: 23663408]
9. Friston K. The free-energy principle: A unified brain theory? Nat Rev Neurosci. 2010; 11:127–138. [PubMed: 20068583]
10. Pezzulo G, Rigoli F, Friston K. Active inference, homeostatic regulation and adaptive behavioural control. Prog Neurobiol. 2015; 134:17–35. [PubMed: 26365173]
11. Barrett LF, Simmons WK. Interoceptive predictions in the brain. Nat Rev Neurosci. 2015; 16:419–429. [PubMed: 26016744]
12. Chanes L, Barrett LF. Redefining the role of limbic areas in cortical processing. Trends in cognitive sciences. 2016; 20:96–106. [PubMed: 26704857]
13. Seth AK. Interoceptive inference, emotion, and the embodied self. Trends in cognitive sciences. 2013; 17:565–573. [PubMed: 24126130]
14. Seth AK, Suzuki K, Critchley HD. An interoceptive predictive coding model of conscious presence. Front Psychol. 2012; 2:1–16.
15. Gu X, FitzGerald TH. Interoceptive inference: Homeostasis and decision-making. Trends in cognitive sciences. 2014; 18:269–270. [PubMed: 24582825]
16. Allen M, Friston KJ. From cognitivism to autopoiesis: Towards a computational framework for the embodied mind. Synthese. 2016:1–24.
17. Craig AD. How do you feel? Interoception: The sense of the physiological condition of the body. Nat Rev Neurosci. 2002; 3:655–666. [PubMed: 12154366]
18. Craig, B. How do you feel?: An interoceptive moment with your neurobiological self. Princeton University Press; 2014.
19. Sherrington, C. Textbook of physiology. Schäfer, EA., editor. Pentland; 1900. p. 920-1001.
20. Sterling, P., Laughlin, S. Principles of neural design. MIT Press; 2015.
21. Sterling P. Allostasis: A model of predictive regulation. Physiol Behav. 2012; 106:5–15. [PubMed: 21684297]

22. McEwen BS, Stellar E. Stress and the individual. Mechanisms leading to disease. Arch Intern Med. 1993; 153:2093–2101. [PubMed: 8379800]
23. Barrett, LF. How emotions are made: The secret life of the brain. Houghton-Mifflin-Harcourt; 2017.
24. Barrett LF. The theory of constructed emotion: An active inference account of interoception and categorization. Soc Cogn Affect Neurosci. 2016
25. Barrett LF, Quigley KS, Hamilton P. An active inference theory of allostasis and interoception in depression. Phil Trans R Soc B. 2016; 371
26. Damasio A, Carvalho GB. The nature of feelings: Evolutionary and neurobiological origins. Nat Rev Neurosci. 2013; 14:143–152. [PubMed: 23329161]
27. Critchley HD, Harrison NA. Visceral influences on brain and behavior. Neuron. 2013; 77:624–638. [PubMed: 23439117]
28. Barrett LF, Satpute AB. Large-scale brain networks in affective and social neuroscience: Towards an integrative functional architecture of the brain. Curr Opin Neurobiol. 2013; 23:361–372. [PubMed: 23352202]
29. Anderson, ML. After phrenology neural reuse and the interactive brain. MIT Press; 2014.
30. Yeo BT, et al. Functional specialization and flexibility in human association cortex. Cereb Cortex. 2015; 25:3654–3672. [PubMed: 25249407]
31. Barbas H, Rempel-Clower N. Cortical structure predicts the pattern of corticocortical connections. Cereb Cortex. 1997; 7:635–646. [PubMed: 9373019]
32. Barbas H. General cortical and special prefrontal connections: Principles from structure to function. Annu Rev Neurosci. 2015; 38:269–289. [PubMed: 25897871]
33. Rempel-Clower NL, Barbas H. The laminar pattern of connections between prefrontal and anterior temporal cortices in the rhesus monkey is related to cortical structure and function. Cereb Cortex. 2000; 10:851–865. [PubMed: 10982746]
34. Medalla M, Barbas H. Specialized prefrontal “auditory fields”: Organization of primate prefrontal-temporal pathways. Front Neurosci. 2014; 8:77. [PubMed: 24795553]
35. Medalla M, Barbas H. Diversity of laminar connections linking periarcuate and lateral intraparietal areas depends on cortical structure. Eur J Neurosci. 2006; 23:161–179. [PubMed: 16420426]
36. Hilgetag CC, Grant S. Cytoarchitectural differences are a key determinant of laminar projection origins in the visual cortex. Neuroimage. 2010; 51:1006–1017. [PubMed: 20211270]
37. Goulas A, Uylings HB, Stiers P. Mapping the hierarchical layout of the structural network of the macaque prefrontal cortex. Cereb Cortex. 2014; 24:1178–1194. [PubMed: 23258344]
38. Bastos AM, et al. Canonical microcircuits for predictive coding. Neuron. 2012; 76:695–711. [PubMed: 23177956]
39. Adams RA, Stephan KE, Brown HR, Frith CD, Friston KJ. The computational anatomy of psychosis. Front Psychiatry. 2013; 4:47. [PubMed: 23750138]
40. Shipp S, Adams RA, Friston KJ. Reflections on agranular architecture: Predictive coding in the motor cortex. Trends Neurosci. 2013; 36:706–716. [PubMed: 24157198]
41. Weston CS. Another major function of the anterior cingulate cortex: The representation of requirements. Neurosci Biobehav Rev. 2012; 36:90–110. [PubMed: 21554898]
42. Vogt BA. Pain and emotion interactions in subregions of the cingulate gyrus. Nat Rev Neurosci. 2005; 6:533–544. [PubMed: 15995724]
43. Ongur D, An X, Price JL. Prefrontal cortical projections to the hypothalamus in macaque monkeys. J Comp Neurol. 1998; 401:480–505. [PubMed: 9826274]
44. Vogt BA, Vogt L, Farber NB, Bush G. Architecture and neurocytology of monkey cingulate gyrus. J Comp Neurol. 2005; 485:218–239. [PubMed: 15791645]
45. Nieuwenhuys R. The insular cortex: A review. Prog Brain Res. 2012; 195:123–163. [PubMed: 22230626]
46. Avery JA, et al. A common gustatory and interoceptive representation in the human mid-insula. Hum Brain Mapp. 2015; 36:2996–3006. [PubMed: 25950427]
47. Hutchison RM, Everling S. Monkey in the middle: Why non-human primates are needed to bridge the gap in resting-state investigations. Front Neuroanat. 2012; 6:29. [PubMed: 22855672]

48. Deco G, Jirsa VK, McIntosh AR. Emerging concepts for the dynamical organization of resting-state activity in the brain. Nat Rev Neurosci. 2011; 12:43–56. [PubMed: 21170073]
49. Cohen AL, et al. Defining functional areas in individual human brains using resting functional connectivity mri. Neuroimage. 2008; 41:45–57. [PubMed: 18367410]
50. Raichle ME. The brain's default mode network. Annu Rev Neurosci. 2015; 38:433–447. [PubMed: 25938726]
51. Touroutoglou A, Hollenbeck M, Dickerson BC, Barrett LF. Dissociable large-scale networks anchored in the right anterior insula subserve affective experience and attention. Neuroimage. 2012; 60:1947–1958. [PubMed: 22361166]
52. Seeley WW, et al. Dissociable intrinsic connectivity networks for salience processing and executive control. J Neurosci. 2007; 27:2349–2356. [PubMed: 17329432]
53. Dosenbach NU, Fair DA, Cohen AL, Schlaggar BL, Petersen SE. A dual-networks architecture of top-down control. Trends in cognitive sciences. 2008; 12:99–105. [PubMed: 18262825]
54. Corbetta M, Shulman GL. Control of goal-directed and stimulus-driven attention in the brain. Nat Rev Neurosci. 2002; 3:201–215. [PubMed: 11994752]
55. Yeo BT, et al. The organization of the human cerebral cortex estimated by intrinsic functional connectivity. J Neurophysiol. 2011; 106:1125–1165. [PubMed: 21653723]
56. Nieuwenhuys, R., Voogd, J., Huijzen, Cv. The human central nervous system. Vol. Ch. 8. Springer; 2008. p. 253-279.
57. Brooks JC, Faull OK, Pattinson KT, Jenkinson M. Physiological noise in brainstem fmri. Front Hum Neurosci. 2013; 7:623. [PubMed: 24109446]
58. Craig AD. How do you feel--now? The anterior insula and human awareness. Nat Rev Neurosci. 2009; 10:59–70. [PubMed: 19096369]
59. Ongur D, Price JL. The organization of networks within the orbital and medial prefrontal cortex of rats, monkeys and humans. Cereb Cortex. 2000; 10:206–219. [PubMed: 10731217]
60. Hoistad M, Barbas H. Sequence of information processing for emotions through pathways linking temporal and insular cortices with the amygdala. Neuroimage. 2008; 40:1016–1033. [PubMed: 18261932]
61. Lang, PJ., Bradley, MM., Cuthbert, BN. Technical Report A-8. University of Florida; Gainesville, FL: 2008. International affective picture system (iaps): Affective ratings of pictures and instruction manual.
62. Moriguchi Y, et al. Differential hemodynamic response in affective circuitry with aging: An fmri study of novelty, valence, and arousal. J Cogn Neurosci. 2011; 23:1027–1041. [PubMed: 20521849]
63. Weierich MR, Wright CI, Negreira A, Dickerson BC, Barrett LF. Novelty as a dimension in the affective brain. Neuroimage. 2010; 49:2871–2878. [PubMed: 19796697]
64. Damasio, AR. Descartes' error: Emotion, reason, and the human brain. Putnam; 1994.
65. Wiens S, Mezzacappa ES, Katkin ES. Heartbeat detection and the experience of emotions. Cognition and Emotion. 2000; 14:417–427.
66. Barrett LF, Quigley KS, Bliss-Moreau E, Aronson KR. Interoceptive sensitivity and self-reports of emotional experience. J Pers Soc Psychol. 2004; 87:684–697. [PubMed: 15535779]
67. Dunn BD, et al. Listening to your heart: How interoception shapes emotion experience and intuitive decision making. Psychol Sci. 2010; 21:1835–1844. [PubMed: 21106893]
68. Whitehead WE, Drescher VM, Heiman P, Blackwell B. Relation of heart rate control to heartbeat perception. Biofeedback and Self-Regulation. 1977; 2:371–392.
69. Schandry R. Heart beat perception and emotional experience. Psychophysiology. 1981; 18:483–488. [PubMed: 7267933]
70. Kleckner IR, Wormwood JB, Simmons WK, Barrett LF, Quigley KS. Methodological recommendations for a heartbeat detection-based measure of interoceptive sensitivity. Psychophysiology. 2015; 52:1432–1440. [PubMed: 26265009]
71. Khalsa SS, Rudrauf D, Feinstein JS, Tranel D. The pathways of interoceptive awareness. Nat Neurosci. 2009; 12:1494–1496. [PubMed: 19881506]

72. Lindquist KA, Barrett LF. A functional architecture of the human brain: Emerging insights from the science of emotion. Trends in cognitive sciences. 2012; 16:533–540. [PubMed: 23036719]
73. van den Heuvel MP, Sporns O. Rich-club organization of the human connectome. J Neurosci. 2011; 31:15775–15786. [PubMed: 22049421]
74. McIntosh AR. Contexts and catalysts: A resolution of the localization and integration of function in the brain. Neuroinformatics. 2004; 2:175–182. [PubMed: 15319515]
75. Beissner F, Schumann A, Brunn F, Eisentrager D, Bar KJ. Advances in functional magnetic resonance imaging of the human brainstem. Neuroimage. 2014; 86:91–98. [PubMed: 23933038]
76. Bar KJ, et al. Functional connectivity and network analysis of midbrain and brainstem nuclei. Neuroimage. 2016; 134:53–63. [PubMed: 27046112]
77. Edlow BL, McNab JA, Witzel T, Kinney HC. The structural connectome of the human central homeostatic network. Brain Connect. 2016; 6:187–200. [PubMed: 26530629]
78. Dum RP, Levinthal DJ, Strick PL. Motor, cognitive, and affective areas of the cerebral cortex influence the adrenal medulla. Proc Natl Acad Sci U S A. 2016; 113:9922–9927. [PubMed: 27528671]
79. Blessing, WW., Benarroch, EE. The human nervous system. Mai, JK., Paxinos, G., editors. Academic Press; 2012. p. 1058-1073.
80. Simmons WK, et al. Keeping the body in mind: Insula functional organization and functional connectivity integrate interoceptive, exteroceptive, and emotional awareness. Hum Brain Mapp. 2012; 000
81. Margulies DS, et al. Mapping the functional connectivity of anterior cingulate cortex. Neuroimage. 2007; 37:579–588. [PubMed: 17604651]
82. Bickart KC, Dickerson BC, Barrett LF. The amygdala as a hub in brain networks that support social life. Neuropsychologia. 2014; 63:235–248. [PubMed: 25152530]
83. Smith DV, Clithero JA, Boltuck SE, Huettel SA. Functional connectivity with ventromedial prefrontal cortex reflects subjective value for social rewards. Soc Cogn Affect Neurosci. 2014; 9:2017–2025. [PubMed: 24493836]
84. van den Heuvel MP, Kahn RS, Goni J, Sporns O. High-cost, high-capacity backbone for global brain communication. Proc Natl Acad Sci U S A. 2012; 109:11372–11377. [PubMed: 22711833]
85. van den Heuvel MP, Sporns O. An anatomical substrate for integration among functional networks in human cortex. J Neurosci. 2013; 33:14489–14500. [PubMed: 24005300]
86. Mesulam MM. From sensation to cognition. Brain. 1998; 121:1013–1052. [PubMed: 9648540]
87. Zold CL, Hussain Shuler MG. Theta oscillations in visual cortex emerge with experience to convey expected reward time and experienced reward rate. J Neurosci. 2015; 35:9603–9614. [PubMed: 26134643]
88. Satpute AB, et al. Involvement of sensory regions in affective experience: A meta-analysis. Front Psychol. 2015; 6:1860. [PubMed: 26696928]
89. Vuilleumier P. How brains beware: Neural mechanisms of emotional attention. Trends in cognitive sciences. 2005; 9:585–594. [PubMed: 16289871]
90. Allen M, et al. Anterior insula coordinates hierarchical processing of tactile mismatch responses. Neuroimage. 2016; 127:34–43. [PubMed: 26584870]
91. Sun FW, et al. Youthful brains in older adults: Preserved neuroanatomy in the default mode and salience networks contributes to youthful memory in superaging. J Neurosci. 2016; 36:9659–9668. [PubMed: 27629716]
92. Barrett LF, Bliss-Moreau E. Affect as a psychological primitive. Advances in Experimental Social Psychology. 2009; 41:167–218. [PubMed: 20552040]
93. Barrett, LF. How emotions are made: The secret life the brain. Houghton-Mifflin-Harcourt; 2017.
94. Barrett LF, Russell JA. Structure of current affect: Controversies and emerging consensus. Current Directions in Psychological Science. 1999; 8:10–14.
95. Kuppens P, Tuerlinckx F, Russell JA, Barrett LF. The relation between valence and arousal in subjective experience. Psychol Bull. 2013; 139:917–940. [PubMed: 23231533]
96. Damasio, AR. The feeling of what happens: Body and emotion in the making of consciousness. Houghton Mifflin Harcourt; 1999.

97. Dreyfus, G., Thompson, E. The cambridge handbook of consciousness. Zelazo, Philip DavidMoscovitch, Morris, Thompson, Evan, editors. Cambridge University Press; 2007. p. 89-114.

98. Edelman, GM., Tononi, G. A universe of consciousness: How matter becomes imagination. Basic books; 2000.

99. James, W. The principles of psychology. Vol. 1. Dover; 1890/2007.

100. Searle, JR. The rediscovery of the mind. MIT press; 1992.

101. Searle, JR. Mind: A brief introduction. Oxford University Press; 2004.

102. Wundt, W. Outlines of psychology. Wilhelm Engelmann; 1897.

103. Fodor, JA. The modularity of mind: An essay on faculty psychology. MIT press; 1983.

104. Li D, Christ SE, Cowan N. Domain-general and domain-specific functional networks in working memory. Neuroimage. 2014; 102(Pt 2):646–656. [PubMed: 25178986]

105. Fuster, JM. Cell Press; 2000.

106. Kayser C, Petkov CI, Augath M, Logothetis NK. Functional imaging reveals visual modulation of specific fields in auditory cortex. J Neurosci. 2007; 27:1824–1835. [PubMed: 17314280]

107. Liang M, Mouraux A, Hu L, Iannetti GD. Primary sensory cortices contain distinguishable spatial patterns of activity for each sense. Nature communications. 2013; 4:1979.

108. Edelman GM, Gally JA. Degeneracy and complexity in biological systems. Proceedings of the National Academy of Sciences. 2001; 98:13763–13768.

109. Tong Y, et al. Systemic low-frequency oscillations in bold signal vary with tissue type. Front Neurosci. 2016; 10:313. [PubMed: 27445680]

110. Satpute AB, et al. Identification of discrete functional subregions of the human periaqueductal gray. Proc Natl Acad Sci U S A. 2013; 110:17101–17106. [PubMed: 24082116]

111. Murphy K, Birn RM, Handwerker DA, Jones TB, Bandettini PA. The impact of global signal regression on resting state correlations: Are anti-correlated networks introduced? Neuroimage. 2009; 44:893–905. [PubMed: 18976716]

112. Raz G, et al. Functional connectivity dynamics during film viewing reveal common networks for different emotional experiences. Cogn Affect Behav Neurosci. 2016

113. Morrison SF. Differential control of sympathetic outflow. Am J Physiol Regul Integr Comp Physiol. 2001; 281:R683–698. [PubMed: 11506981]

114. Buckner RL. The serendipitous discovery of the brain's default network. Neuroimage. 2012; 62:1137–1145. [PubMed: 22037421]

115. Mesulam M. The evolving landscape of human cortical connectivity: Facts and inferences. Neuroimage. 2012; 62:2182–2189. [PubMed: 22209814]

116. Hassabis D, Maguire EA. The construction system of the brain. Philos Trans R Soc Lond B Biol Sci. 2009; 364:1263–1271. [PubMed: 19528007]

117. Power JD, et al. Functional network organization of the human brain. Neuron. 2011; 72:665–678. [PubMed: 22099467]

118. Menon V, Uddin LQ. Saliency, switching, attention and control: A network model of insula function. Brain structure & function. 2010; 214:655–667. [PubMed: 20512370]

119. Li SS, McNally GP. The conditions that promote fear learning: Prediction error and pavlovian fear conditioning. Neurobiol Learn Mem. 2014; 108:14–21. [PubMed: 23684989]

120. Barrett, LF. How emotions are made: The new science of the mind and brain. Houghton-Mifflin-Harcourt; 2016.

121. Guidi M, Huber L, Lampe L, Gauthier CJ, Moller HE. Lamina-dependent calibrated bold response in human primary motor cortex. Neuroimage. 2016; 141:250–261. [PubMed: 27364473]

122. Crossley NA, et al. The hubs of the human connectome are generally implicated in the anatomy of brain disorders. Brain. 2014; 137:2382–2395. [PubMed: 25057133]

123. Goodkind M, et al. Identification of a common neurobiological substrate for mental illness. JAMA psychiatry. 2015; 72:305–315. [PubMed: 25651064]

124. Menon V. Large-scale brain networks and psychopathology: A unifying triple network model. Trends in cognitive sciences. 2011; 15:483–506. [PubMed: 21908230]
125. Harshaw C. Interoceptive dysfunction: Toward an integrated framework for understanding somatic and affective disturbance in depression. Psychol Bull. 2015; 141:311–363. [PubMed: 25365763]
126. Paulus MP, Stein MB. Interoception in anxiety and depression. Brain Structure Function. 2010; 214:451–463. [PubMed: 20490545]
127. Naqvi NH, Bechara A. The insula and drug addiction: An interoceptive view of pleasure, urges, and decision-making. Brain Structure Function. 2010; 214:435–450. [PubMed: 20512364]
128. Farmer MA, Baliki MN, Apkarian AV. A dynamic network perspective of chronic pain. Neurosci Lett. 2012; 520:197–203. [PubMed: 22579823]
129. Mayer EA. Gut feelings: The emerging biology of gut-brain communication. Nat Rev Neurosci. 2011; 12:453–466. [PubMed: 21750565]
130. Radley J, Morilak D, Viau V, Campeau S. Chronic stress and brain plasticity: Mechanisms underlying adaptive and maladaptive changes and implications for stress-related cns disorders. Neurosci Biobehav Rev. 2015; 58:79–91. [PubMed: 26116544]
131. Gianaros PJ, Wager TD. Brain-body pathways linking psychological stress and physical health. Curr Dir Psychol Sci. 2015; 24:313–321. [PubMed: 26279608]
132. Gefen T, et al. Morphometric and histologic substrates of cingulate integrity in elders with exceptional memory capacity. J Neurosci. 2015; 35:1781–1791. [PubMed: 25632151]
133. Rogalski EJ, et al. Youthful memory capacity in old brains: Anatomic and genetic clues from the northwestern superaging project. J Cogn Neurosci. 2013; 25:29–36. [PubMed: 23198888]
134. Angevaren M, Aufdemkampe G, Verhaar HJ, Aleman A, Vanhees L. Physical activity and enhanced fitness to improve cognitive function in older people without known cognitive impairment. Cochrane Database Syst Rev. 2008:CD005381.
135. Farb N, et al. Interoception, contemplative practice, and health. Front Psychol. 2015; 6:763. [PubMed: 26106345]
136. Tang YY, Holzel BK, Posner MI. The neuroscience of mindfulness meditation. Nat Rev Neurosci. 2015; 16:213–225. [PubMed: 25783612]
137. Thombs BD, et al. Prevalence of depression in survivors of acute myocardial infarction. J Gen Intern Med. 2006; 21:30–38. [PubMed: 16423120]
138. Moreno-Smith M, Lutgendorf SK, Sood AK. Impact of stress on cancer metastasis. Future Oncol. 2010; 6:1863–1881. [PubMed: 21142861]
139. Kolodny A, et al. The prescription opioid and heroin crisis: A public health approach to an epidemic of addiction. Annu Rev Public Health. 2015; 36:559–574. [PubMed: 25581144]
140. Turecki G, Brent DA. Suicide and suicidal behaviour. Lancet. 2016; 387:1227–1239. [PubMed: 26385066]
141. Buckner RL, Krienen FM, Castellanos A, Diaz JC, Yeo BT. The organization of the human cerebellum estimated by intrinsic functional connectivity. J Neurophysiol. 2011; 106:2322–2345. [PubMed: 21795627]
142. Touroutoglou A, Andreano JM, Barrett LF, Dickerson BC. Brain network connectivity-behavioral relationships exhibit trait-like properties: Evidence from hippocampal connectivity and memory. Hippocampus. 2015
143. Kramer JH, et al. Nih examiner: Conceptualization and development of an executive function battery. J Int Neuropsychol Soc. 2014; 20:11–19. [PubMed: 24103232]
144. Bradley MM, Lang PJ. Measuring emotion: The self-assessment manikin and the semantic differential. J Behav Ther Exp Psychiatry. 1994; 25:49–59. [PubMed: 7962581]
145. Jo HJ, et al. Effective preprocessing procedures virtually eliminate distance-dependent motion artifacts in resting state fmri. J Appl Math. 2013; 2013
146. Power JD, Barnes KA, Snyder AZ, Schlaggar BL, Petersen SE. Spurious but systematic correlations in functional connectivity mri networks arise from subject motion. Neuroimage. 2012; 59:2142–2154. [PubMed: 22019881]

147. Tucholka A, Fritsch V, Poline JB, Thirion B. An empirical comparison of surface-based and volume-based group studies in neuroimaging. Neuroimage. 2012; 63:1443–1453. [PubMed: 22732555]

148. Cronbach LJ, Rajaratnam N, Gleser GC. Theory of generalizability: A liberalization of reliability theory. British Journal of Statistical Psychology. 1963; 16:137–163.

149. Boucsein W, et al. Publication recommendations for electrodermal measurements. Psychophysiology. 2012; 49:1017–1034. [PubMed: 22680988]

150. Schell AM, Dawson ME, Filion DL. Psychophysiological correlates of electrodermal lability. Psychophysiology. 1988; 25:619–632. [PubMed: 3241850]

151. Xia C, Touroutoglou A, Quigley KS, Barrett LF, Dickerson BC. Salience network connectivity modulates skin conductance responses in predicting arousal experience. J Cogn Neurosci. 2016

152. Fredrikson M, et al. Functional neuroanatomical correlates of electrodermal activity: A positron emission tomographic study. Psychophysiology. 1998; 35:179–185. [PubMed: 9529944]

153. Bohus B, et al. The neurobiology of the central nucleus of the amygdala in relation to neuroendocrine and autonomic outflow. Prog Brain Res. 1996; 107:447–460. [PubMed: 8782536]

154. Mufson EJ, Mesulam MM, Pandya DN. Insular interconnections with the amygdala in rhesus monkey. Neuroscience. 1981; 6:1231–1248. [PubMed: 6167896]

155. Mufson EJ, Mesulam MM. Insula of the old world monkey. Ii: Afferent cortical input and comments on the claustrum. J Comp Neurol. 1982; 212:23–37. [PubMed: 7174906]

156. Ghashghaei HT, Hilgetag CC, Barbas H. Sequence of information processing for emotions based on the anatomic dialogue between prefrontal cortex and amygdala. Neuroimage. 2007; 34:905–923. [PubMed: 17126037]

157. Morecraft RJ, et al. Cytoarchitecture and cortical connections of the anterior cingulate and adjacent somatomotor fields in the rhesus monkey. Brain Res Bull. 2012; 87:457–497. [PubMed: 22240273]

158. Mesulam MM, Mufson EJ. Insula of the old world monkey. Iii: Efferent cortical output and comments on function. J Comp Neurol. 1982; 212:38–52. [PubMed: 7174907]

159. Cavdar S, et al. The afferent connections of the posterior hypothalamic nucleus in the rat using horseradish peroxidase. J Anat. 2001; 198:463–472. [PubMed: 11327208]

160. An X, Bandler R, Ongur D, Price JL. Prefrontal cortical projections to longitudinal columns in the midbrain periaqueductal gray in macaque monkeys. J Comp Neurol. 1998; 401:455–479. [PubMed: 9826273]

161. Saper CB. Reciprocal parabrachial-cortical connections in the rat. Brain Res. 1982; 242:33–40. [PubMed: 7104731]

162. Saper CB. Convergence of autonomic and limbic connections in the insular cortex of the rat. J Comp Neurol. 1982; 210:163–173. [PubMed: 7130477]

163. Fudge JL, Breitbart MA, Danish M, Pannoni V. Insular and gustatory inputs to the caudal ventral striatum in primates. J Comp Neurol. 2005; 490:101–118. [PubMed: 16052493]

164. Carmichael ST, Price JL. Connectional networks within the orbital and medial prefrontal cortex of macaque monkeys. J Comp Neurol. 1996; 371:179–207. [PubMed: 8835726]

165. Aggleton JP, Burton MJ, Passingham RE. Cortical and subcortical afferents to the amygdala of the rhesus monkey (macaca mulatta). Brain Res. 1980; 190:347–368. [PubMed: 6768425]

166. Stefanacci L, Amaral DG. Some observations on cortical inputs to the macaque monkey amygdala: An anterograde tracing study. J Comp Neurol. 2002; 451:301–323. [PubMed: 12210126]

167. Chikama M, McFarland NR, Amaral DG, Haber SN. Insular cortical projections to functional regions of the striatum correlate with cortical cytoarchitectonic organization in the primate. J Neurosci. 1997; 17:9686–9705. [PubMed: 9391023]

168. Chiba T, Kayahara T, Nakano K. Efferent projections of infralimbic and prelimbic areas of the medial prefrontal cortex in the japanese monkey, macaca fuscata. Brain Res. 2001; 888:83–101. [PubMed: 11146055]

169. Vogt BA, Pandya DN. Cingulate cortex of the rhesus monkey: Ii. Cortical afferents. J Comp Neurol. 1987; 262:271–289. [PubMed: 3624555]

170. Rempel-Clower NL, Barbas H. Topographic organization of connections between the hypothalamus and prefrontal cortex in the rhesus monkey. J Comp Neurol. 1998; 398:393–419. [PubMed: 9714151]

171. Freedman LJ, Insel TR, Smith Y. Subcortical projections of area 25 (subgenual cortex) of the macaque monkey. J Comp Neurol. 2000; 421:172–188. [PubMed: 10813780]

172. Terreberry RR, Neafsey EJ. Rat medial frontal cortex: A visceral motor region with a direct projection to the solitary nucleus. Brain Res. 1983; 278:245–249. [PubMed: 6315155]

173. van der Kooy D, McGinty JF, Koda LY, Gerfen CR, Bloom FE. Visceral cortex: A direct connection from prefrontal cortex to the solitary nucleus in rat. Neurosci Lett. 1982; 33:123–127. [PubMed: 6185887]

174. Room P, Russchen FT, Groenewegen HJ, Lohman AH. Efferent connections of the prelimbic (area 32) and the infralimbic (area 25) cortices: An anterograde tracing study in the cat. J Comp Neurol. 1985; 242:40–55. [PubMed: 4078047]

175. Pandya DN, Van Hoesen GW, Mesulam MM. Efferent connections of the cingulate gyrus in the rhesus monkey. Exp Brain Res. 1981; 42:319–330. [PubMed: 6165607]

176. Vogt, BA., Palomero-Gallagher, N. The human central nervous system. Mai, JK., Paxinos, G., editors. Vol. Ch. 25. Elsevier; 2012. p. 943-987.

177. Haber SN, Kim KS, Mailly P, Calzavara R. Reward-related cortical inputs define a large striatal region in primates that interface with associative cortical connections, providing a substrate for incentive-based learning. J Neurosci. 2006; 26:8368–8376. [PubMed: 16899732]

178. Price JL, Amaral DG. An autoradiographic study of the projections of the central nucleus of the monkey amygdala. J Neurosci. 1981; 1:1242–1259. [PubMed: 6171630]

179. Fudge JL, Kunishio K, Walsh P, Richard C, Haber SN. Amygdaloid projections to ventromedial striatal subterritories in the primate. Neuroscience. 2002; 110:257–275. [PubMed: 11958868]

180. Morecraft RJ, Van Hoesen GW. Convergence of limbic input to the cingulate motor cortex in the rhesus monkey. Brain Res Bull. 1998; 45:209–232. [PubMed: 9443842]

181. Saleem KS, Kondo H, Price JL. Complementary circuits connecting the orbital and medial prefrontal networks with the temporal, insular, and opercular cortex in the macaque monkey. J Comp Neurol. 2008; 506:659–693. [PubMed: 18067141]

182. Barbas H, Ghashghaei H, Dombrowski SM, Rempel-Clower NL. Medial prefrontal cortices are unified by common connections with superior temporal cortices and distinguished by input from memory-related areas in the rhesus monkey. J Comp Neurol. 1999; 410:343–367. [PubMed: 10404405]

183. Ongur D, Ferry AT, Price JL. Architectonic subdivision of the human orbital and medial prefrontal cortex. J Comp Neurol. 2003; 460:425–449. [PubMed: 12692859]

184. Ghaziri J, et al. The corticocortical structural connectivity of the human insula. Cereb Cortex. 2015

185. Wiech K, Jbabdi S, Lin CS, Andersson J, Tracey I. Differential structural and resting state connectivity between insular subdivisions and other pain-related brain regions. Pain. 2014; 155:2047–2055. [PubMed: 25047781]

186. Gianaros PJ, Sheu LK. A review of neuroimaging studies of stressor-evoked blood pressure reactivity: Emerging evidence for a brain-body pathway to coronary heart disease risk. Neuroimage. 2009; 47:922–936. [PubMed: 19410652]

187. Kurth F, Zilles K, Fox PT, Laird AR, Eickhoff SB. A link between the systems: Functional differentiation and integration within the human insula revealed by meta-analysis. Brain structure & function. 2010; 214:519–534. [PubMed: 20512376]

188. Gianaros PJ, et al. An inflammatory pathway links atherosclerotic cardiovascular disease risk to neural activity evoked by the cognitive regulation of emotion. Biol Psychiatry. 2014; 75:738–745. [PubMed: 24267410]

189. Wager TD, et al. Brain mediators of cardiovascular responses to social threat: Part i: Reciprocal dorsal and ventral sub-regions of the medial prefrontal cortex and heart-rate reactivity. Neuroimage. 2009; 47:821–835. [PubMed: 19465137]

190. Harper RM, et al. Fmri responses to cold pressor challenges in control and obstructive sleep apnea subjects. J Appl Physiol (1985). 2003; 94:1583–1595. [PubMed: 12514164]
191. Gianaros PJ, et al. Individual differences in stressor-evoked blood pressure reactivity vary with activation, volume, and functional connectivity of the amygdala. J Neurosci. 2008; 28:990–999. [PubMed: 18216206]
192. Zilles, K., Amunts, K. The human central nervous system. Mai, JK., Paxinos, G., editors. Vol. Ch. 23. Elsevier; 2012. p. 836-895.
193. Petrides, M., Pandya, DN. The human central nervous system. Mai, JK., Paxinos, G., editors. Vol. Ch. 26. Elsevier; 2012. p. 988-1011.
194. Barbas H. Specialized elements of orbitofrontal cortex in primates. Ann N Y Acad Sci. 2007; 1121:10–32. [PubMed: 17698996]
195. Mesulam MM, Mufson EJ. Insula of the old world monkey. I Architectonics in the insulo-orbito-temporal component of the paralimbic brain. J Comp Neurol. 1982; 212:1–22. [PubMed: 7174905]
196. Yarkoni T. Big correlations in little studies: Inflated fmri correlations reflect low statistical power-commentary on vul et al (2009). Perspect Psychol Sci. 2009; 4:294–298. [PubMed: 26158966]
197. Wilson-Mendenhall CD, Barrett LF, Simmons WK, Barsalou LW. Grounding emotion in situated conceptualization. Neuropsychologia. 2011; 49:1105–1127. [PubMed: 21192959]
198. Wilson-Mendenhall CD, Barrett LF, Barsalou LW. Variety in emotional life: Within-category typicality of emotional experiences is associated with neural activity in large-scale brain networks. Soc Cogn Affect Neurosci. 2015; 10:62–71. [PubMed: 24563528]
199. Kober H, et al. Functional grouping and cortical-subcortical interactions in emotion: A meta-analysis of neuroimaging studies. Neuroimage. 2008; 42:998–1031. [PubMed: 18579414]
200. Skerry AE, Saxe R. Neural representations of emotion are organized around abstract event features. Curr Biol. 2015; 25:1945–1954. [PubMed: 26212878]
201. Clithero JA, Rangel A. Informatic parcellation of the network involved in the computation of subjective value. Soc Cogn Affect Neurosci. 2014; 9:1289–1302. [PubMed: 23887811]
202. Bickart KC, Hollenbeck MC, Barrett LF, Dickerson BC. Intrinsic amygdala-cortical functional connectivity predicts social network size in humans. J Neurosci. 2012; 32:14729–14741. [PubMed: 23077058]
203. Baliki MN, Mansour AR, Baria AT, Apkarian AV. Functional reorganization of the default mode network across chronic pain conditions. PLoS One. 2014; 9:e106133. [PubMed: 25180885]
204. Schurz M, Radua J, Aichhorn M, Richlan F, Perner J. Fractionating theory of mind: A meta-analysis of functional brain imaging studies. Neurosci Biobehav Rev. 2014; 42:9–34. [PubMed: 24486722]
205. Morelli SA, Lieberman MD. The role of automaticity and attention in neural processes underlying empathy for happiness, sadness, and anxiety. Front Hum Neurosci. 2013; 7:160. [PubMed: 23658538]
206. Chiong W, et al. The salience network causally influences default mode network activity during moral reasoning. Brain. 2013; 136:1929–1941. [PubMed: 23576128]
207. Liu X, Hairston J, Schrier M, Fan J. Common and distinct networks underlying reward valence and processing stages: A meta-analysis of functional neuroimaging studies. Neurosci Biobehav Rev. 2011; 35:1219–1236. [PubMed: 21185861]
208. Engelmann JM, et al. Neural substrates of smoking cue reactivity: A meta-analysis of fmri studies. Neuroimage. 2012; 60:252–262. [PubMed: 22206965]
209. Schacter DL, Addis DR. The cognitive neuroscience of constructive memory: Remembering the past and imagining the future. Philos Trans R Soc Lond B Biol Sci. 2007; 362:773–786. [PubMed: 17395575]
210. Bar M, Aminoff E, Mason M, Fenske M. The units of thought. Hippocampus. 2007; 17:420–428. [PubMed: 17455334]
211. Fernandino L, et al. Concept representation reflects multimodal abstraction: A framework for embodied semantics. Cereb Cortex. 2016; 26:2018–2034. [PubMed: 25750259]

212. Touroutoglou A, Lindquist KA, Dickerson BC, Barrett LF. Intrinsic connectivity in the human brain does not reveal networks for 'basic' emotions. Soc Cogn Affect Neurosci. 2015; 10:1257–1265. [PubMed: 25680990]

213. Dhanjal NS, Wise RJ. Frontoparietal cognitive control of verbal memory recall in alzheimer's disease. Ann Neurol. 2014; 76:241–251. [PubMed: 24933580]

214. Dosenbach NU, et al. Distinct brain networks for adaptive and stable task control in humans. Proc Natl Acad Sci U S A. 2007; 104:11073–11078. [PubMed: 17576922]

215. Ansell EB, Rando K, Tuit K, Guarnaccia J, Sinha R. Cumulative adversity and smaller gray matter volume in medial prefrontal, anterior cingulate, and insula regions. Biol Psychiatry. 2012; 72:57–64. [PubMed: 22218286]

216. Caseras X, et al. Anatomical and functional overlap within the insula and anterior cingulate cortex during interoception and phobic symptom provocation. Hum Brain Mapp. 2013; 34:1220–1229. [PubMed: 22162203]

217. Wolf DH, et al. Striatal intrinsic reinforcement signals during recognition memory: Relationship to response bias and dysregulation in schizophrenia. Front Behav Neurosci. 2011; 5:81. [PubMed: 22355285]

218. Grady CL, Luk G, Craik FI, Bialystok E. Brain network activity in monolingual and bilingual older adults. Neuropsychologia. 2015; 66:170–181. [PubMed: 25445783]

219. Derbyshire SW, Whalley MG, Stenger VA, Oakley DA. Cerebral activation during hypnotically induced and imagined pain. Neuroimage. 2004; 23:392–401. [PubMed: 15325387]

220. Feldstein Ewing SW, Filbey FM, Sabbineni A, Chandler LD, Hutchison KE. How psychosocial alcohol interventions work: A preliminary look at what fmri can tell us. Alcohol Clin Exp Res. 2011; 35:643–651. [PubMed: 21223301]

221. Singer T, et al. Empathy for pain involves the affective but not sensory components of pain. Science. 2004; 303:1157–1162. [PubMed: 14976305]

222. Kirk U, Downar J, Montague PR. Interoception drives increased rational decision-making in meditators playing the ultimatum game. Front Neurosci. 2011; 5:49. [PubMed: 21559066]

223. FitzGerald TH, Schwartenbeck P, Dolan RJ. Reward-related activity in ventral striatum is action contingent and modulated by behavioral relevance. J Neurosci. 2014; 34:1271–1279. [PubMed: 24453318]

224. Fernandino L, Humphries CJ, Conant L, Seidenberg MS, Binder JR. Heteromodal cortical areas encode sensory-motor features of word meaning. J Neuroscience. 2016; 36:9763–9769. [PubMed: 27656016]

225. Hermans EJ, et al. Stress-related noradrenergic activity prompts large-scale neural network reconfiguration. Science. 2011; 334:1151–1153. [PubMed: 22116887]

226. Clark-Polner, E., Wager, TD., Satpute, AB., Barrett, LF. The handbook of emotion. Barrett, LF.Lewis, M., Haviland-Jones, JM., editors. Guilford; 2016. p. 146-165.

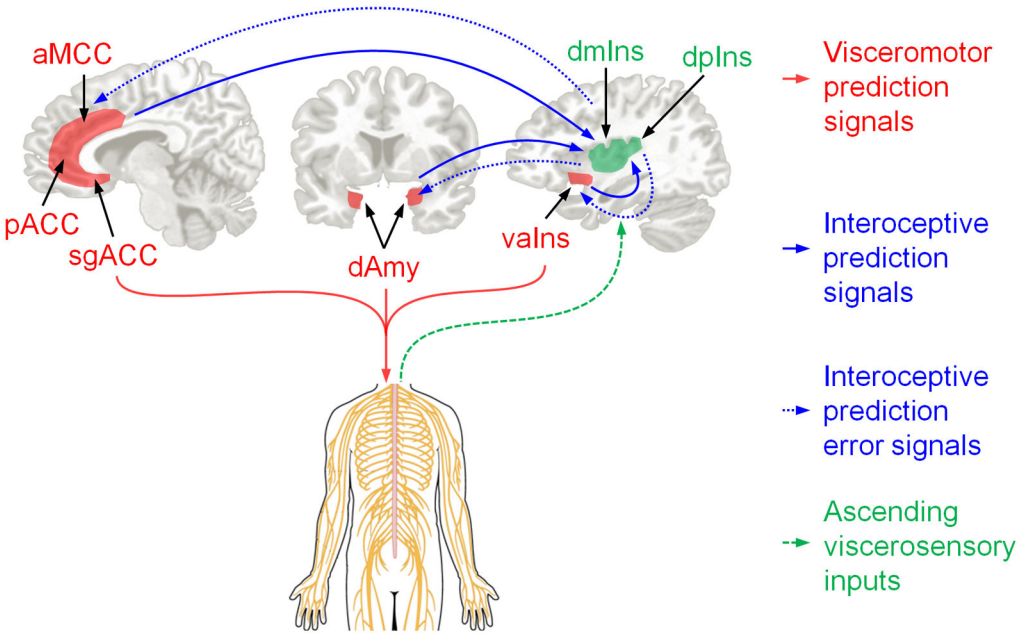

Fig 1.

We identified key visceromotor cortical regions (in red) that provide cortical control the body's internal milieu, including the anterior mid cingulate cortex (aMCC; also called dorsal anterior cingulate cortex (dACC), e.g., [41,42]), pregenual anterior cingulate cortex (pACC), subgenual anterior cingulate cortex (sgACC; for a review of the cingulate, see [176]), and the ventral anterior insula (vaIns; also called agranular insula[43,183] or posterior orbitofrontal cortex[194]); these regions have a less-developed laminar structure (i.e., they are agranular or dysgranular[32,176]). We also included the dorsal amygdala because it contains the central nucleus which is also involved in visceromotor control (for a review, see [153]). Primary interoceptive cortex spans the dorsal mid insula (dmIns) to the dorsal posterior insula (dpIns)[17] along a dysgranular to granular[195] gradient (green regions). Barrett & Simmons (2015) summarized preliminary tract-tracing evidence, supporting the EPIC model[11], that allostasis and interoception are maintained within an integrated system involving limbic cortices (in red) that initiate visceromotor directions to the hypothalamus and brainstem nuclei (e.g., periaqueductal gray, parabrachial nucleus, nucleus of the solitary tract; citations in Table 2) to regulate the autonomic, neuroendocrine, and immune systems (red paths). These visceromotor control regions (less developed laminar organization) also send anticipated sensory consequences of visceromotor changes (as interoceptive prediction signals) to primary interoceptive cortex (more-developed laminar organization; solid blue paths). The incoming sensory inputs from the internal milieu of the body are carried along the vagus nerve and small diameter C and Aδ fibers (dashed green paths) to primary interoceptive cortex in the dorsal sector of the mid to posterior insula (for a review, see [17]); comparisons between prediction signals and ascending sensory input results in interoceptive prediction error. Current interoceptive predictions can be updated by passing prediction error signals to visceromotor regions (dashed blue paths); prediction errors are learning signals and also adjust subsequent predictions. (For simplicity, ascending feedback to visceromotor regions is not shown). aMCC = anterior midcingulate cortex; dAmy = dorsal amygdala;

dmIns = dorsal mid insula; dpIns = dorsal posterior insula; pACC = pregenual anterior cingulate cortex; sgACC = subgenual anterior cingulate cortex; vaIns = ventral anterior insula.

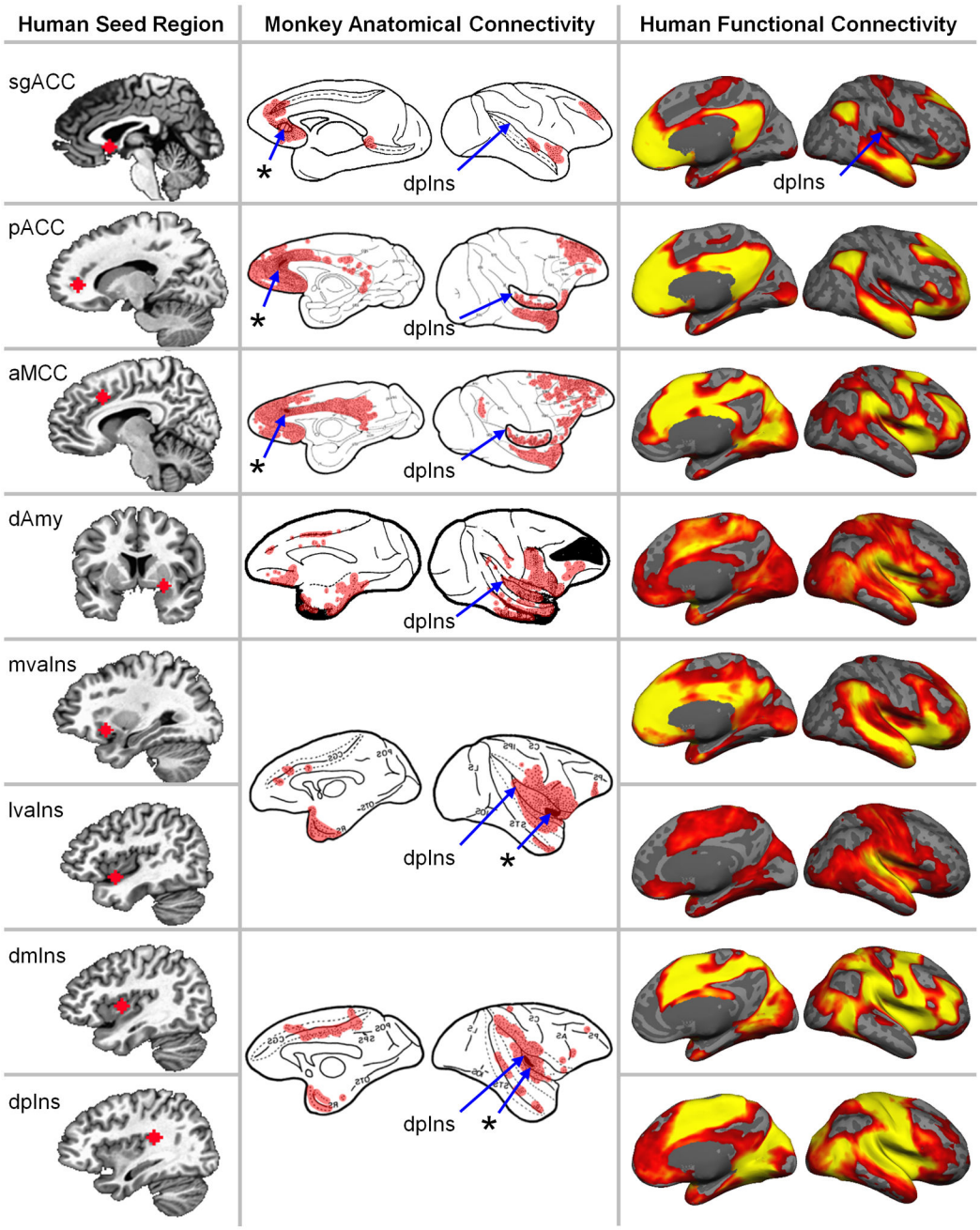

Fig. 2.

Eight regions (“seeds”) used to estimate the unified allostasis/interoceptive system connecting the cortical and amygdalar visceromotor regions and primary interoceptive regions. The left column shows the “seed” region for each discovery map on a human brain template. The middle column summarizes the anatomical connectivity derived from anterograde and/or retrograde tracers injected in macaque brains at a location homologous to the human seed (asterisks with blue arrows). The right column shows the human intrinsic connectivity discovery maps depicting all voxels whose time course is correlated with the seed’s (ranging from $p < 10^{-5}$ in red to $p < 10^{-40}$ in yellow, uncorrected, $N = 280$). To avoid

Type I and Type II errors, which are enhanced with the use of stringent statistical thresholds[196], we opted to separate signal from random noise using replication, according to the mathematics of classical measurement theory[148]. These results replicated in a second sample, $N = 270$ participants, indicating that they are reliable and cannot be attributed to random error (Supplementary Figure 1). Functional connectivity to the entire amygdala and other subcortical regions are shown in Fig. 4. Tract tracing figures were adapted with permission as follows: subgenual anterior cingulate cortex (sgACC) via retrograde tracers in Fig 1 of Vogt & Pandya (1987)[169], pregenual ACC (pACC) via retrograde tracers in Fig 5 of Morecraft, et al. (2012)[157], anterior midcingulate cortex (aMCC) via retrograde tracers in Fig 7 of Morecraft, et al. (2012)[157], dorsal amygdala (dAmy) via retrograde tracers in Fig 3 of Aggleton, et al. (1980)[165], medial ventral anterior insula (mvaIns) and lateral ventral anterior insula (lvaIns) via anterograde tracers in Fig 1 of Mesulam & Mufson (1982)[158], dorsal mid insula (dmIns) and dorsal posterior insula (dpIns) via anterograde tracers in Fig 3 of Mesulam & Mufson (1982)[158]. The monkey anatomical connectivity figures were colored red to visualize results and some were mirrored to match the orientation of the human brain maps. The figures from Morecraft, et al. (2012)[157] were adapted to show the insula in its lateral view.

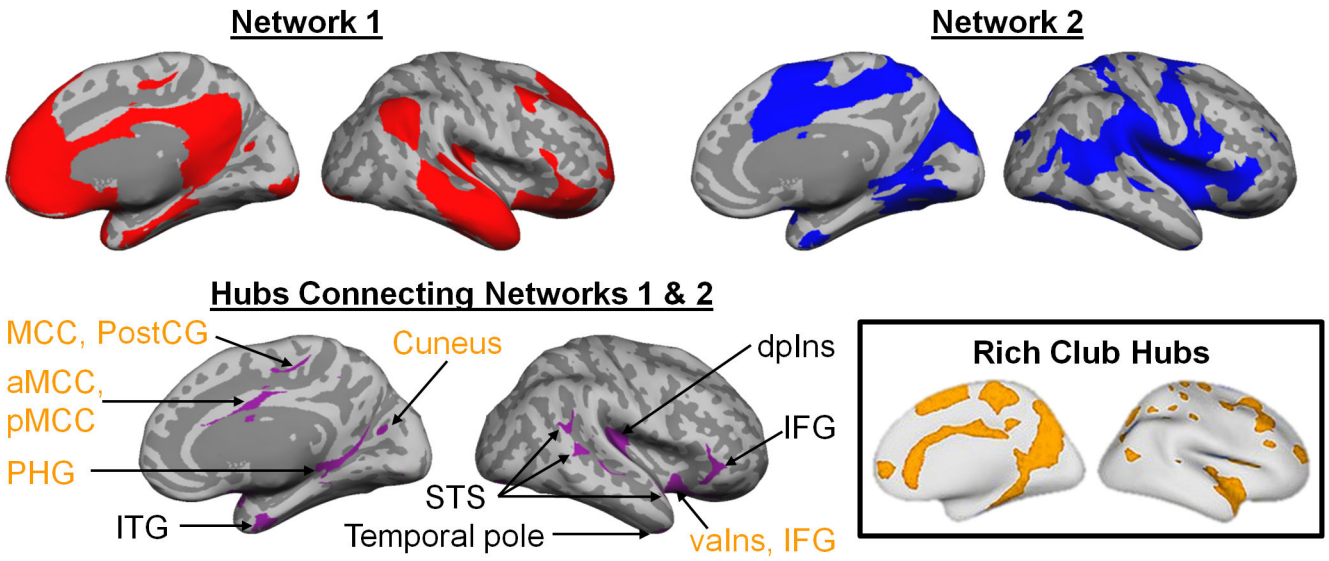

Fig. 3.

The unified allostatic/interoceptive system is composed of two large-scale intrinsic networks (shown in red and blue) that share several hubs (shown in purple; for coordinates, see Supplementary Table 4). Hubs belonging to the "rich club" are shown in yellow. Rich club hubs figure adapted with permission from van den Heuval & Sporns (2013)[85]. All maps result from the sample of 280 participants binarized at $p < 10^{-5}$ uncorrected from a one-sample two-tailed t-test. These results replicated in a second sample, $N = 270$ participants, indicating that they are reliable and cannot be attributed to random error (Supplementary Figure 2). aMCC = anterior midcingulate cortex; dAmy = dorsal amygdala; dpIns = dorsal posterior insula; dmIns = dorsal mid insula; IFG = inferior frontal gyrus; ITG = inferior temporal gyrus; lvaIns = lateral ventral anterior insula; MCC = midcingulate cortex; mvaIns = medial ventral anterior insula; pACC = pregenual anterior cingulate cortex; PHG = parahippocampal gyrus; pMCC = posterior midcingulate cortex; PostCG = postcentral gyrus; sgACC = subgenual anterior cingulate cortex; STS = superior temporal sulcus.

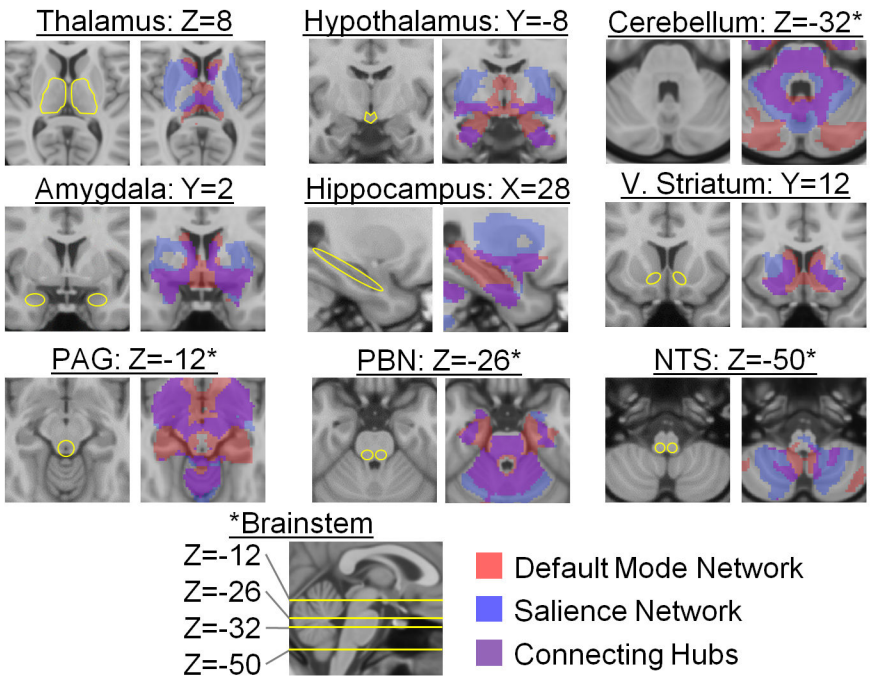

Fig. 4.

Subcortical connectivity of the two integrated intrinsic networks within the allostatic/interoceptive system ($N = 280$; $p < 0.05$ uncorrected). These results replicated in a second sample of $N = 270$ (Supplementary Figure 5). PAG = periaqueductal gray; PBN = parabrachial nucleus; V. Striatum = ventral striatum; NTS = nucleus of the solitary tract.

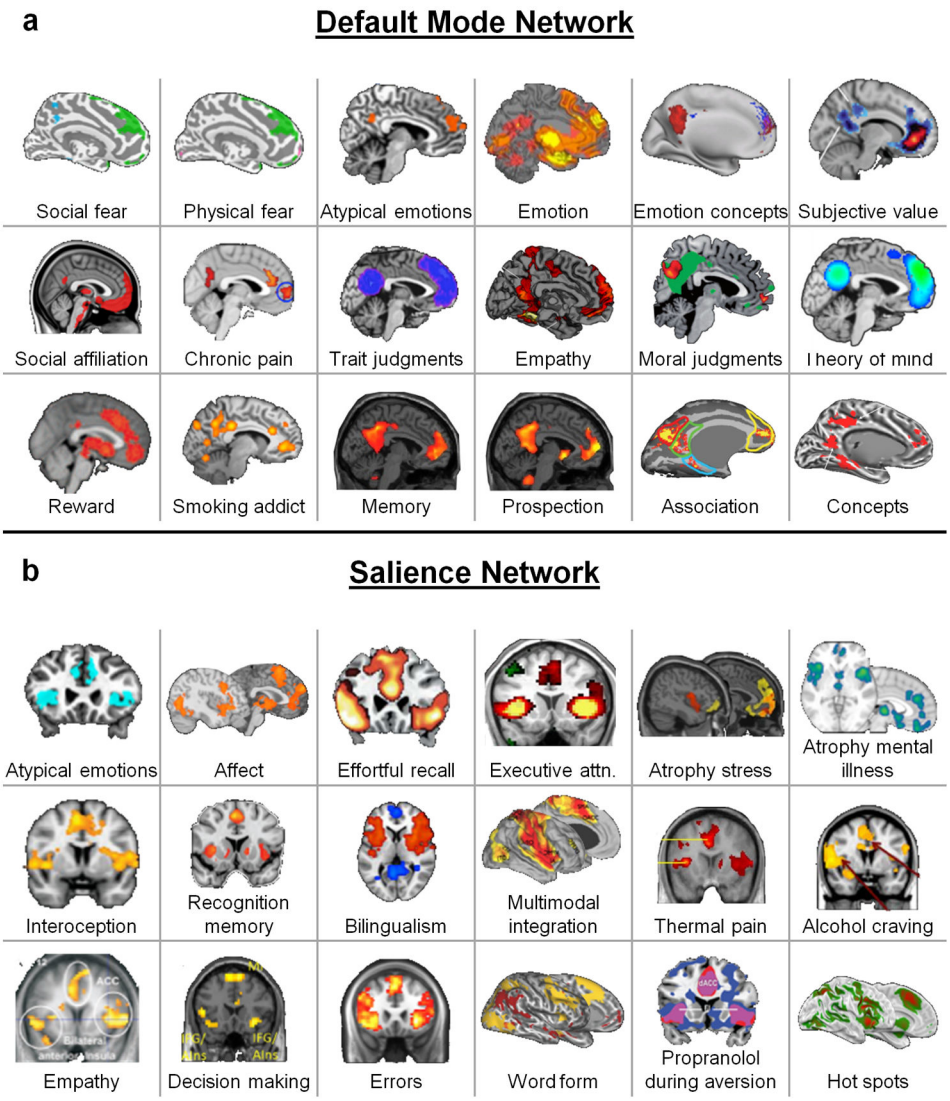

Fig. 5.

The default mode and salience networks each support a wide array of psychological functions, as evidenced by a literature review of psychological or other states that are sensitive to functional or structural features of these networks. These results are consistent with the idea that the default mode and salience networks are domain-general networks that support interoception and allostasis, which we propose are key processes that contribute to all psychological functions. Each sub-figure shows a set of results from an independent study, with citations as follows. Default mode network: Social fear[197], Physical fear[197], Atypical emotions[198], Emotion[199], Emotion concepts[200], Subjective value[201], Social affiliation[202], Chronic pain[203], Trait judgments[204], Empathy[205], Moral judgments[206], Theory of mind[204], Reward[207], Smoking addiction[208], Memory[209], Prospection[209], Association[210], and Concepts[211]. Salience network: Atypical emotion[198], Affect[212], Effortful recall[213], Executive attention[214], Atrophy and stress (chronic yellow, current red)[215], Atrophy and mental illness[123], Interoception[216], Recognition memory[217], Bilingualism[218], Multimodal integration[1], Thermal pain[219], Alcohol craving[220],

Empathy[221], Decision making[222], Errors[223], Word form (yellow)[224], Propranolol during aversion[225], and Hot spots[226].

Table 1

Summary of this study's hypotheses, predictions or questions, and results.

Embodied Predictive Interoception Coding (EPIC) Hypothesis	Experimental Prediction	Result in the Current Study
Interoception and visceromotor control are part of a unified brain system that supports allostasis (Fig 1)	Primary interoceptive cortex (e.g., dorsal mid/posterior insula) is anatomically and functionally connected to agranular and dysgranular visceromotor hubs of the cortex (e.g., sgACC, pACC, aMCC)	• The interoceptive and visceromotor hubs are anatomically connected in monkeys (Table 2) • The interoception and visceromotor hubs are functionally connected in humans (Fig. 2, Supplementary Table 1) • Coordinates for human hubs are show in Table 3
	The allostatic/interoceptive system also includes subcortical and brainstem visceromotor regions.	• Previously established subcortical and brainstem visceromotor regions (e.g., hypothalamus, periaqueductal gray) are part of the unified system for allostasis/ interoception (Fig. 4, Supplementary Figure 6)
	The allostatic/interoceptive brain system contains limbic cortices.	• The allostatic/interoceptive system comprises two established large scale brain networks that contain the majority of limbic cortices: the salience network and the default mode networks (Fig. 3, Supplementary Figure 3)
	Connectivity in the allostatic/interoceptive system is related to an implicit performance measure of interoception in humans	• The correspondence between sympathetic arousal (electrodermal activity) and experienced arousal during an allostatically challenging task is related to functional connectivity within the allostatic/interoceptive system in humans (Supplementary Figure 8)
The allostatic/interoceptive system is domain-general.	The allostatic/interoceptive system sits at the core of the brain's computational architecture.	• Many hubs of the allostatic/interoceptive system have been previously identified as members of the "rich club," which are the most densely connected within the brain and therefore help constitute the brain's "neural backbone" for coordinating neural synchrony (Fig. 3, Supplementary Table 4)
	Brain activity and connectivity in the allostatic/ interoceptive system is associated with a variety of psychological functions	• Both the default mode network and the salience network support a variety of mental phenomena across major psychological domains (e.g., cognition, emotion, perception, and action; Fig. 5)

Other hypotheses, such as the computational dynamics of the proposed allostatic/interoceptive network are beyond the scope of this study. ACC = anterior cingulate cortex; aMCC = anterior midcingulate cortex; dmIns = dorsal mid insula; dpIns = dorsal posterior insula; pACC = pregenual anterior cingulate cortex; sgACC = subgenual anterior cingulate cortex.

Nat Hum Behav. Author manuscript; available in PMC 2017 October 24.

Table 2

Summary of tract-tracing study results in non-human animals, demonstrating anatomical connections between cortical visceromotor and primary interoceptive sensory regions, as well as between cortical and non-cortical visceromotor regions.

	Primary Interoceptive Cortex	Visceromotor Regions				Subcortical and Brainstem Visceromotor Structures	
	To dpIns/dmIns	**To vaIns**	**To sgACC (BA 25)**	**To pACC (BA 24, 32)**	**To aMCC (BA 24)**	**To Amygdala**	**To other subcortical and brainstem regions[a]**
From dpIns/dmIns	-	Case A, Fig 1[155]	Not evident[b]	Case 1, Fig 5[157]	Case B, Fig 3[158]	Case 2, Fig 3[154] Case BB-B, Fig 1[60]	Hypothalamus (rat)[159] PAG: not observed[160] PBN (rat)[161,162] V. Striatum [163] NTS (rat)[162]
From vaIns[c]	Case C, Fig 4[155] Case A, Fig 1[158]	-	Case OM20, Fig 8[164]	Case 1, Fig 5[157]	Case 2, Fig 6[157] Case A, Fig 1[158]	Case A, Fig 1[158] Case 103, Fig 3[165] Fig 2, Table 2[166]	Hypothalamus[43] PAG[160] PBN (rat)[161] V. striatum[167] NTS (rat)[162]
From sgACC (BA 25)	Not evident[d]	Case M707[168]	-	Case 1, Fig 5[157] Fig 2A[169]	Case 3, Fig 7[157] Fig 3A[169]	Case 103, Fig 3[165] Fig 5[156]	Hypothalamus[154,170,171] PAG[160,171] PBN [171] Striatum [171] NTS (rat)[172,173]
From pACC (BA 24, 32)	Not evident[d]	Case M776[168]	Fig 1[169]	-	Case 3, Fig 7[157] Fig 3A[169]	Case 103, Fig 3[165] Fig 5[156]	Hypothalamus[43], PAG[160] PBN (cat)[174] V. striatum (cat)[174] NTS (rat)[173]
From aMCC (BA 24)	Case C, Fig 4[155]	Case A, Fig 1[155]	Case 3, Fig 4[175]	Case 1, Fig 5[157] Fig 2A[169]	-	Case 103, Fig 3[165] Fig 5[156]	Hypothalamus[43] PAG[160] PBN: not present[176] V. striatum[177] NTS (rat)[172]
From Amygdala	Case C, Fig 4[155] Lateral basal nucleus; Case 5, Fig 6[154]	Case A, Fig 1[155] Case 4, Fig 5[154]	Fig 6[156]	Fig 13[169]	Fig 6[156]	-	Hypothalamus[43], PAG[160] PBN[178] V. striatum[179] NTS[178]

Note. Connectivity evidence is in monkeys unless otherwise indicated (e.g., rats, cats). Some connections from dpIns/dmIns to the NTS are unclear due to ambiguity in how Saper (1982)[162] reported subregions of the insula.

[a]We did not assess for projections from subcortical and brainstem regions to cortical regions because we only wanted to determine if the cortical regions support visceromotor control.

[b] Connection from dpIns/dmIns to sgACC not evident in several monkey studies that have the potential to show them (e.g., [158,169,180–182]).

[c] The medial portion of the vaIns exhibits connectivity with subcortical and brainstem regions, but not the lateral portion of the vaIns[43,183].

[d] Connection from sgACC to dpIns/dmIns and from pACC to dpIns/dmIns not evident in several monkey studies that have the potential to show them (e.g., [155,168,180,181]), although weak, direct connectivity is evident in a recent tractography study in humans (Ghaziri, et al., 2015[184], Figure 5). Moreover, connections between sgACC, pACC, and dpIns have been observed in intrinsic functional connectivity analyses in humans (e.g., Fig. 6 of [185]). The discrepancy between human findings and the tract tracing studies in monkeys failing to show connectivity might reflect an expansion of Brodmann area (BA) 24 anterior and ventral to the corpus callosum in humans relative to monkeys and/or the presence of connections between BAs 25/32 and the posterior insula in humans that do not exist in monkeys (Evrard, H. personal communication, December 27, 2015).

BA = Brodmann area; aMCC = anterior midcingulate cortex; dmIns = dorsal mid insula; dpIns = dorsal posterior insula; NTS = nucleus of the solitary tract; PAG = periaqueductal gray; PBN = parabrachial nucleus; pACC = pregenual anterior cingulate cortex; sgACC = subgenual anterior cingulate cortex; V. striatum = ventral striatum.

Table 3

Seeds used for intrinsic connectivity analyses.

Seed	Type of region predicted by EPIC model	Cortical Lamination	MNI Coordinates
dpIns	Primary interoceptive cortex	Granular	36, −32, 16[186]
dmIns	Primary interoceptive cortex	Dysgranular	41, 2, 3[187]
sgACC	Visceromotor control	Agranular	2, 14, −6[188]
pACC	Visceromotor control	Agranular	13, 44, 0[186]
aMCC	Visceromotor control	Agranular	9, 22, 33[189]
mvaIns	Visceromotor control	Agranular	30, 16, −14[190]
lvaIns	Sensory integration	Agranular	44, 6, −15[189]
dAmy	Visceromotor control	N/A	27, 3, −12[191]

Note: All seeds are in the right hemisphere. Evidence for cortical lamination comes from Vogt (2005)[42,192,193].

Each anatomical region of interest was represented by one 4-mm-radius seed except for the ventral anterior insula (vaIns), which required a medial and a lateral seed (mvaIns and lvaIns, respectively) to capture the previously-established functional distinction between the medial visceromotor network (containing mvaIns) and the orbital sensory integration network (containing lvaIns) in the orbitofrontal cortex[183].

aMCC = anterior midcingulate cortex; dAmy = dorsal amygdala; dmIns = dorsal mid insula; dpIns = dorsal posterior insula; lvaIns = lateral ventral anterior insula; mvaIns = medial ventral anterior insula; pACC = pregenual anterior cingulate cortex; sgACC = subgenual anterior cingulate cortex.